

1-1-1972

Optimization of ${}^6\text{Li}$ and ${}^7\text{Li}$ in a fusion blanket

Danny Dean Kloock
Iowa State University

Follow this and additional works at: <https://lib.dr.iastate.edu/rtd>

 Part of the [Engineering Commons](#)

Recommended Citation

Kloock, Danny Dean, "Optimization of ${}^6\text{Li}$ and ${}^7\text{Li}$ in a fusion blanket" (1972). *Retrospective Theses and Dissertations*. 18178.
<https://lib.dr.iastate.edu/rtd/18178>

This Thesis is brought to you for free and open access by the Iowa State University Capstones, Theses and Dissertations at Iowa State University Digital Repository. It has been accepted for inclusion in Retrospective Theses and Dissertations by an authorized administrator of Iowa State University Digital Repository. For more information, please contact digirep@iastate.edu.

Optimization of ${}^6\text{Li}$ and ${}^7\text{Li}$
in a fusion blanket

by

Danny Dean Kloock

A Thesis Submitted to the
Graduate Faculty in Partial Fulfillment of
The Requirements for the Degree of
MASTER OF SCIENCE

Major: Nuclear Engineering

Signatures have been redacted for privacy

Iowa State University
Ames, Iowa

1972

TABLE OF CONTENTS

	<u>Page</u>
I. INTRODUCTION	1
II. REVIEW OF LITERATURE	3
III. THEORY	6
IV. PROCEDURE	13
A. Microscopic Cross Sections	13
B. Group Macroscopic Cross Sections	30
C. Diffusion Coefficients	35
D. Calculations of Constants for the Diffusion Equation	39
E. Tritium Breeding Rates	40
V. DISCUSSION OF RESULTS	44
VI. SUMMARY AND CONCLUSIONS	54
VII. SUGGESTIONS FOR FURTHER STUDY	55
VIII. LITERATURE CITED	56
IX. ACKNOWLEDGMENTS	58

I. INTRODUCTION

Ever since the possibilities of using deuterium and tritium to fuel a fusion reactor were realized, it has been known that such a reactor could only be practical if more tritium is produced than consumed. Deuterium presents no problem as a fuel since economical means, such as distillation, chemical exchange, or electrolysis, can be used to extract the small amount of naturally occurring deuterium from water. Unlike deuterium, however, tritium does not exist in nature and, therefore, has to be bred from other materials.

Several elements can be used to breed tritium, but lithium is by far the best choice. Lithium has two naturally occurring isotopes, ${}^6\text{Li}$, which is in abundance of 7%, and ${}^7\text{Li}$, which comprises the remainder.

Tritium is bred from lithium in two different ways. One way is by the ${}^6\text{Li}(n, t)$ reaction, which is most prominent at low neutron energies. The other way is by the ${}^7\text{Li}(n, tn)$ reaction, which occurs at high neutron energies. The purpose of this study is to find the optimum concentrations of ${}^6\text{Li}$ and ${}^7\text{Li}$ that will produce the greatest tritium breeding rate.

The method that was used was multi-group neutron diffusion theory. An infinite slab of lithium was used to idealize a breeding blanket for a fusion reactor. The group fluxes were calculated for slabs of 100 cm and 200 cm and for varying concentrations of ${}^6\text{Li}$ and ${}^7\text{Li}$ using the multi-group diffusion code, FAIMOS. Ten groups were incorporated into the code for flux calculations. From the calculated fluxes, the

tritium breeding rate in each group was found and all rates were added together to arrive at a total tritium breeding rate. The total tritium breeding rates were found for different concentrations of ${}^6\text{Li}$ in each slab, and from these calculations an optimum concentration was determined.

It is emphasized that no attempt was made in this study to design or suggest building materials [11, 12]. A process for the concentration of ${}^6\text{Li}$ and an economic analysis of such a process were also not determined. It is hoped that the results of this study could further design techniques of a tritium breeding blanket around a D-T fusion reactor core.

II. REVIEW OF LITERATURE

George Bell of Los Alamos Scientific Laboratory in 1965 investigated the process of breeding tritium from lithium [2]. He approached the problem by using a twenty-five group DSN transport code with cylindrical geometry. Molybdenum was chosen for the container walls because of its excellent refractory properties. Bell utilized the ${}^6\text{Li}(n, t)$ reaction, and for this reason, incorporated beryllium as a moderator in the blanket. Beryllium was chosen because of its ability to moderate the neutrons into lower energy groups where the ${}^6\text{Li}(n, t)$ cross section is greatest, and also because of its $(n, 2n)$ neutron producing reaction. Flibe, $2\text{LiF} \cdot \text{BeF}_2$, was used as the coolant for several reasons. Since pure molten lithium is a fairly good conductor of electricity, problems might arise from its use around the magnetic lines of force used to contain the fusion plasma. Using flibe as a coolant and beryllium as the moderator, a breeding ratio of 1.79 was calculated. Bell concluded the following: (1) the use of fluorine in flibe reduces the breeding ratio; (2) beryllium is a good moderator to use in the blanket; (3) if pure lithium is used, the blanket would be too thick; and (4) flibe is a good coolant.

In 1967, Donald Steiner [14] of Oak Ridge National Laboratory did a similar study using the transport code, ANISN, incorporating 100 groups with slab geometry. Steiner took a slightly different approach, however, making these observations:

- (1) Niobium would be a better material for container walls because of its better welding characteristics.

- (2) Lithium would be a better coolant to use than flibe because of its lower costs and superior heat transfer properties. The lithium coolant channels could be constructed to run parallel to the magnetic field lines containing the plasma and, thereby, minimize the electromagnetic resistance to the flow.
- (3) Although beryllium gives good neutron multiplication and is an excellent moderator, it is very expensive and undergoes severe radiation damage.

Steiner used two different approaches to blanket design. One was to assume, through proper design of coolant channels, that the electromagnetic resistance to the flow could be minimized, and as a result, pure lithium could be used throughout the blanket. The second design was conservative in that flibe was used to cool the inner wall while lithium was used throughout the rest of the blanket.

Through his calculations, Steiner reached these conclusions:

- (1) Very good breeding ratios can be achieved without the use of beryllium as a moderator. This can be explained from the fact that without beryllium the flux is shifted to higher energies. This, of course, decreases the production of tritium from the ${}^6\text{Li}(n, t)$ reaction, but at the same time increases the production of tritium from the ${}^7\text{Li}(n, tn)$ reaction. It must also be remembered that while the ${}^6\text{Li}(n, t)$ reaction completely absorbs the neutron, the ${}^7\text{Li}(n, tn)$ reaction releases another neutron that possibly can go on to produce more tritium.

- (2) If flibe is used rather than lithium, the breeding is considerably reduced. This can be attributed to the inelastic scattering of high energy neutrons by fluorine and results in a reduction of tritium breeding from the high energy ${}^7\text{Li}(n, tn)$ reaction.

Steiner also did an economic analysis of the different blanket designs. The most promising design in this respect seemed to be a blanket of lithium, without beryllium, and niobium rather than molybdenum as container wall material.

III. THEORY

Diffusion theory is an approximation to the more exact transport theory. Diffusion theory does not take into account the angular distribution of the flux, and in this respect, is less exact than transport theory. For certain problems, diffusion theory can provide a good approximation to the more exact transport solution.

Consider an arbitrary volume in which neutrons are diffusing in a steady state condition. The equation that describes the neutron flux at any point r and energy E within the volume is

$$\nabla \cdot D(E)\nabla\phi(r, E) - \Sigma_t(E)\phi(r, E) + S(r, E) = 0, \quad (1)$$

where $D(E)$ is the diffusion coefficient, $\phi(r, E)$ is the neutron flux, $\Sigma_t(E)$ is the total removal cross section, and $S(r, E)$ represents the neutron source.

Because of the energy dependence, Eq. (1) is extremely difficult to use. In order to get Eq. (1) in a useable form, the multi-group diffusion method is incorporated. The central idea behind multi-group diffusion theory is that the entire energy range of the neutrons is divided into energy groups. The neutron balance in group i is then

$$\int_{E_{il}}^{E_{iu}} [\nabla \cdot D(E)\nabla\phi(r, E) - \Sigma_t(E)\phi(r, E) + S(r, E)]dE = 0, \quad (2)$$

where E_{il} and E_{iu} are the lower and upper energy boundaries of group i , respectively. Equation (2) can be simplified by describing the diffusion of neutrons in each energy group by an average group flux given as

$$\begin{aligned}\phi^i(r) &= \frac{\int_{E_{il}}^{E_{iu}} \phi(r, E) dE}{\int_{E_{il}}^{E_{iu}} dE}, \\ &= \frac{\int_i \phi(r, E) dE}{\Delta E_i},\end{aligned}\quad (3)$$

where the integration is over the energy range of group i , and $\Delta E_i = E_{iu} - E_{il}$ is the energy width of group i . The neutron balance in group i can then be given by the multi-group diffusion equation

$$D^i \nabla^2 \phi^i(r) - \Sigma_t^i \phi^i(r) + S^i(r) = 0, \quad (4)$$

where

$$S^i(r) = \frac{\int_i S(r, E) dE}{\Delta E_i},$$

which is the neutron source for group i , and D^i and Σ_t^i are the diffusion coefficient and total removal cross section of group i , respectively, which will be defined in more detail later in this section.

To get Eq. (4) in a more workable form, it is best to look at each term individually. Neutrons can be lost from group i by leakage, which is represented by $D^i \nabla^2 \phi^i(r)$. Also, neutrons can be removed from group i by absorption or scattering, either elastically or inelastically, to lower energy groups. Thus,

$$\Sigma_t^i \phi^i(r) = \left(\Sigma_a^i + \sum_{j=i+1}^N \Sigma_s(i \rightarrow j) \right) \phi^i(r),$$

where $\Sigma_s(i \rightarrow j)$ is the macroscopic scattering (elastic and inelastic) cross section from group i to group j . The summation is over all

energy groups lower than i , and N is the lowest energy group. Neutrons can appear in group i by scattering from higher energy groups or by neutron sources such as fission. Therefore,

$$S^i(r) = \sum_{j=1}^{i-1} (\Sigma_s(j \rightarrow i) \phi^j(r)) + \chi^i \sum_{j=1}^N [(\nu \Sigma_f)^j \phi^j(r)],$$

where $\Sigma_s(j \rightarrow i)$ is the macroscopic scattering cross section into group i from group j with the summation over all energy groups greater than i , $\sum_{j=1}^N [(\nu \Sigma_f)^j \phi^j(r)]$ is the total number of neutrons produced from fission in all groups per cm^3 per second, and χ^i is the fraction of fission neutrons which appear in group i .

Thus, a better and more workable form of Eq. (4) is

$$D^i \nabla^2 \phi^i(r) - \Sigma_a^i \phi^i(r) - \sum_{j=i+1}^N [\Sigma_s(i \rightarrow j)] \phi^j(r) + \sum_{j=1}^{i-1} [\Sigma_s(j \rightarrow i) \phi^j(r)] + \chi^i \sum_{j=1}^N [(\nu \Sigma_f)^j \phi^j(r)] = 0. \quad (5)$$

Equation (5) represents a set of N , second order, coupled, differential equations which must be solved simultaneously.

Before solving Eq. (5), the constants need to be defined. Each of the constants D^i , Σ_a^i , and $(\nu \Sigma_f)^i$ represents an average value in group i , weighted by the flux as a function of energy within each group. Thus, if the flux can be represented by a separable function of space and energy,

$$D^i = \frac{\int_i D(E) \phi(E) dE}{\int_i \phi(E) dE}, \quad (6)$$

where the limits of integration are the lower and upper energy bounds of group i . Likewise,

$$\Sigma_a^i = \frac{\int_i \Sigma_a(E) \phi(E) dE}{\int_i \phi(E) dE} \quad (7)$$

and

$$(\nu \Sigma_f)^i = \frac{\int_i \nu(E) \Sigma_f(E) \phi(E) dE}{\int_i \phi(E) dE} \quad (8)$$

In some instances $\phi(E)$ can be considered constant over the energy group interval [9], and as a result, Eqs. (6), (7), and (8) become

$$D^i = \frac{\int_i D(E) dE}{\Delta E_i}, \quad (9)$$

$$\Sigma_a^i = \frac{\int_i \Sigma_a(E) dE}{\Delta E_i}, \quad (10)$$

and

$$(\nu \Sigma_f)^i = \frac{\int_i \nu(E) \Sigma_f(E) dE}{\Delta E_i}, \quad (11)$$

where ΔE_i is the energy width of group i . The constant $\chi^i = \int_i \chi(E) dE$, where $\chi(E)$ is the prompt neutron spectrum normalized so that $\int_0^\infty \chi(E) d(E) = 1$.

The transfer coefficients, $\Sigma_s(i \rightarrow j)$, can be defined in different ways, depending upon how the groups are chosen. Probably the simplest way is to choose the groups such that neutrons from one energy group can only be scattered into the next lowest energy group. In this respect the groups are directly coupled. Thus, we have $\Sigma_s(i \rightarrow j) = 0$, for $j > i + 1$. The criterion to calculate $\Sigma_s(i \rightarrow i + 1)$ can be illustrated by the use of Fig. 1. In order that groups $i - 1$ and i be

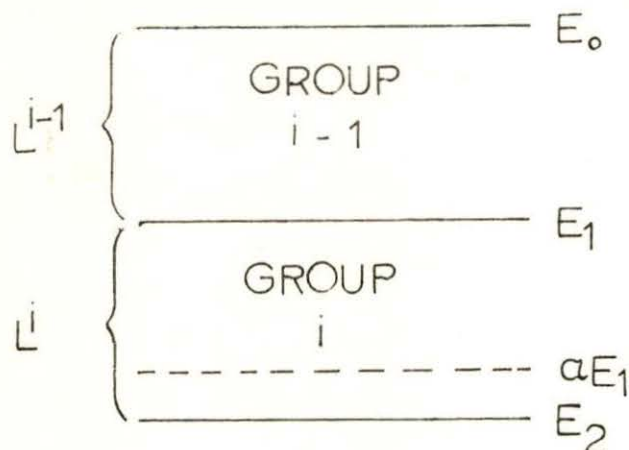


Fig. 1. Criterion for direct coupling of groups.

directly coupled, a neutron in group $i - 1$ cannot be scattered past E_2 . This condition can be met if

$$L^i > \ln \frac{E}{\alpha E_1} - \ln \frac{E}{E_1} \\ > \ln \frac{1}{\alpha},$$

where L^i is the lethargy width of group i and α is the maximum fractional amount of energy a neutron can lose in a single collision. Alpha can be calculated from $\alpha = [(A - 1)/(A + 1)]^2$, where A is the atomic mass of the diffusing material. If this criterion is met, the transfer coefficients can be calculated in the following way. The total number of scattering collisions in group i per cm^3 per second is $\Sigma_s^i \phi^i(r)$, where

$$\Sigma_s^i = \frac{\int_i \Sigma_s(E) \phi(E) dE}{\int_i \phi(E) d(E)} \approx \frac{\int_i \Sigma_s(E) dE}{\Delta E_i}.$$

If $\bar{\xi}^i$ is the average increase in lethargy per collision, then it takes $L^i/\bar{\xi}^i$ collisions to traverse the i th energy group. Here,

$$\bar{\xi}^i = \frac{1}{\Sigma_s^i} \sum_l \xi_l \Sigma_{sl}^i,$$

where the summation over l represents different nuclear species, and

$$\xi_l = 1 + \frac{\alpha}{1 - \alpha} \ln \alpha.$$

In terms of A ,

$$\xi_l = 1 - \frac{(A - 1)^2}{2A} \ln \left(\frac{A + 1}{A - 1} \right).$$

Therefore, there will be $\bar{\xi}^i \Sigma_s^i \phi(r) / L^i$ neutrons per cm^3 per second leaving group i and entering group $i + 1$, or

$$\Sigma_s(i \rightarrow i + 1) = \frac{\bar{\xi}^i \Sigma_s^i}{L^i}. \quad (12)$$

When more than one or two energy groups are used, Eq. (5) can be solved by use of a computer. FAIMOS [3], a one-dimensional, neutron diffusion code, is used to solve Eq. (5). Basically, the code solves the equation,

$$-D^i \nabla^2 \phi^i(r) + \Sigma_t^i \phi^i(r) = \chi^i S(r) + \sum_{j=q}^{i-1} [\Sigma_s(j \rightarrow i) \phi^j(r)],$$

where D^i is the diffusion coefficient in each group,

$$\Sigma_t^i = \Sigma_a^i + D^i (B^2)^i + t^i \Sigma_p^{\text{th}} + \sum_{j=i+1}^g \Sigma_s(i \rightarrow j),$$

Σ_a^i is the absorption cross section in each group, $(B^2)^i$ is the transverse buckling in each group, Σ_p^{th} is the poison cross section in

the thermal group, t^i is the ratio of the poison cross section in group i to the poison cross section in the thermal group, $\Sigma_s(i \rightarrow j)$ is the transfer coefficients from group i into group j , g is the minimum of 18 or $i + 8$, q is the maximum of 1 or $i - 8$, χ^i is the integral of the fission spectrum over the energy range of group i , and $S(r)$ is the fission source normalized so that one neutron is produced in the entire fissionable volume. Thus,

$$S(r) = \frac{\sum_{i=1}^{18} (\nu\Sigma_f)^i \phi^i(r)}{\lambda},$$

where

$$\lambda = \int_V \sum_{i=1}^{18} (\nu\Sigma_f)^i \phi^i(r) dr,$$

and V is the fissionable volume.

A description of the finite difference equations and how they are used in FAIMOS can be found in reference [1]. Also, a complete description of the input formats to be used in FAIMOS are given in reference [3].

FAIMOS is designed so that a microscopic cross section library cannot be used. As a result, macroscopic cross sections must be put into the code. The following section describes how the macroscopic cross sections and other inputs into FAIMOS were formulated.

IV. PROCEDURE

A. Microscopic Cross Sections

Following are described the microscopic cross sectional data for ${}^6\text{Li}$ and ${}^7\text{Li}$ as the cross sections vary with energy. It might be pointed out that the cross sections presented here do not include all of the reactions possible with either isotope of lithium. There is, for example, a ${}^6\text{Li}(n, 2n)$ reaction at about 14.1 MeV. Since this reaction only appears at very high energy levels and is small, about 70 mb, compared with other reactions, about 500 mb, the ${}^6\text{Li}(n, 2n)$ cross section was ignored. Due to its small value of approximately 10 mb, the ${}^6\text{Li}(n, p)$ reaction was also ignored. With ${}^7\text{Li}$, above 10 MeV an $(n, 2n)$ and an (n, d) reaction were also ignored because of their small values of approximately 50 mb and 10 mb, respectively [6, 13].

The scattering cross sections for both ${}^6\text{Li}$ and ${}^7\text{Li}$ are treated in the following manner. The total scattering cross section, which includes both elastic and inelastic scattering, is treated entirely as elastic scattering. This may seem at first to be a poor assumption, but upon close examination of the scattering cross sections (see Figs. 4 and 5), it can be seen that the total scattering is entirely elastic until approximately 1 MeV. From 1 MeV to 15 MeV, the elastic scattering differs only a few tenths of a barn from the total scattering cross section. Thus, to ease calculations, the assumption was made that scattering from either isotope of lithium will be entirely elastic. Below 0.1 MeV, the ${}^6\text{Li}$ and ${}^7\text{Li}$ total microscopic scattering cross

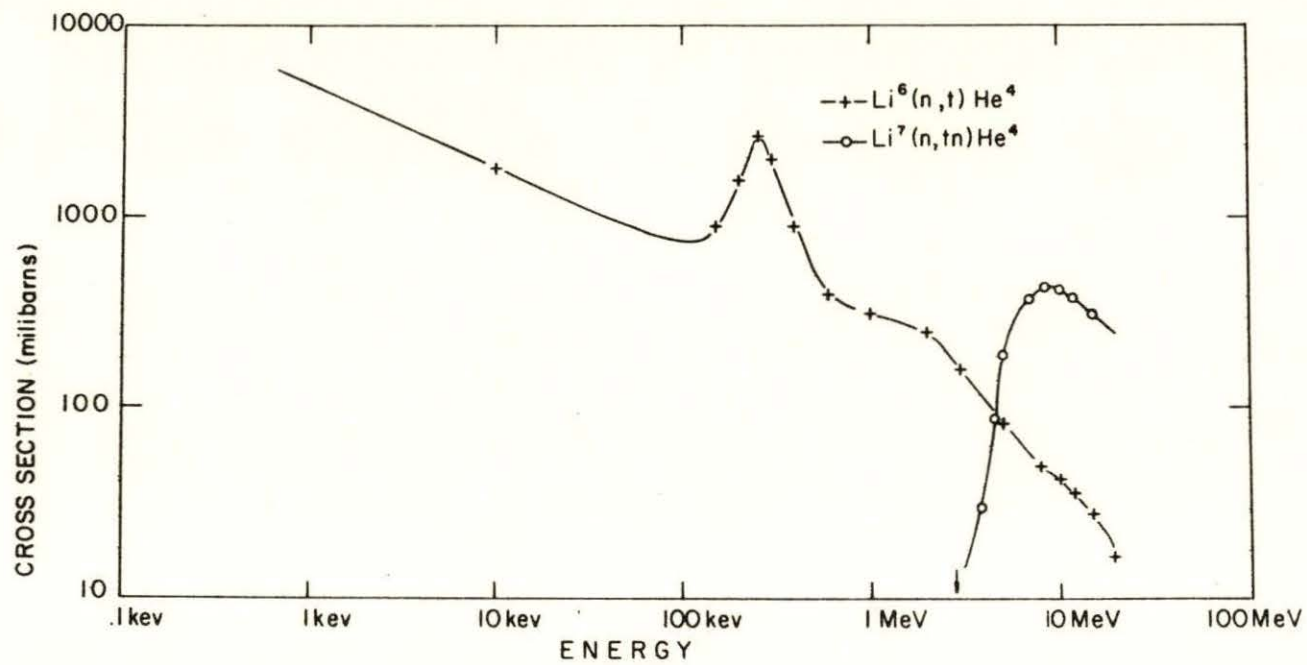


Fig. 2. Microscopic cross sections for production of tritium.

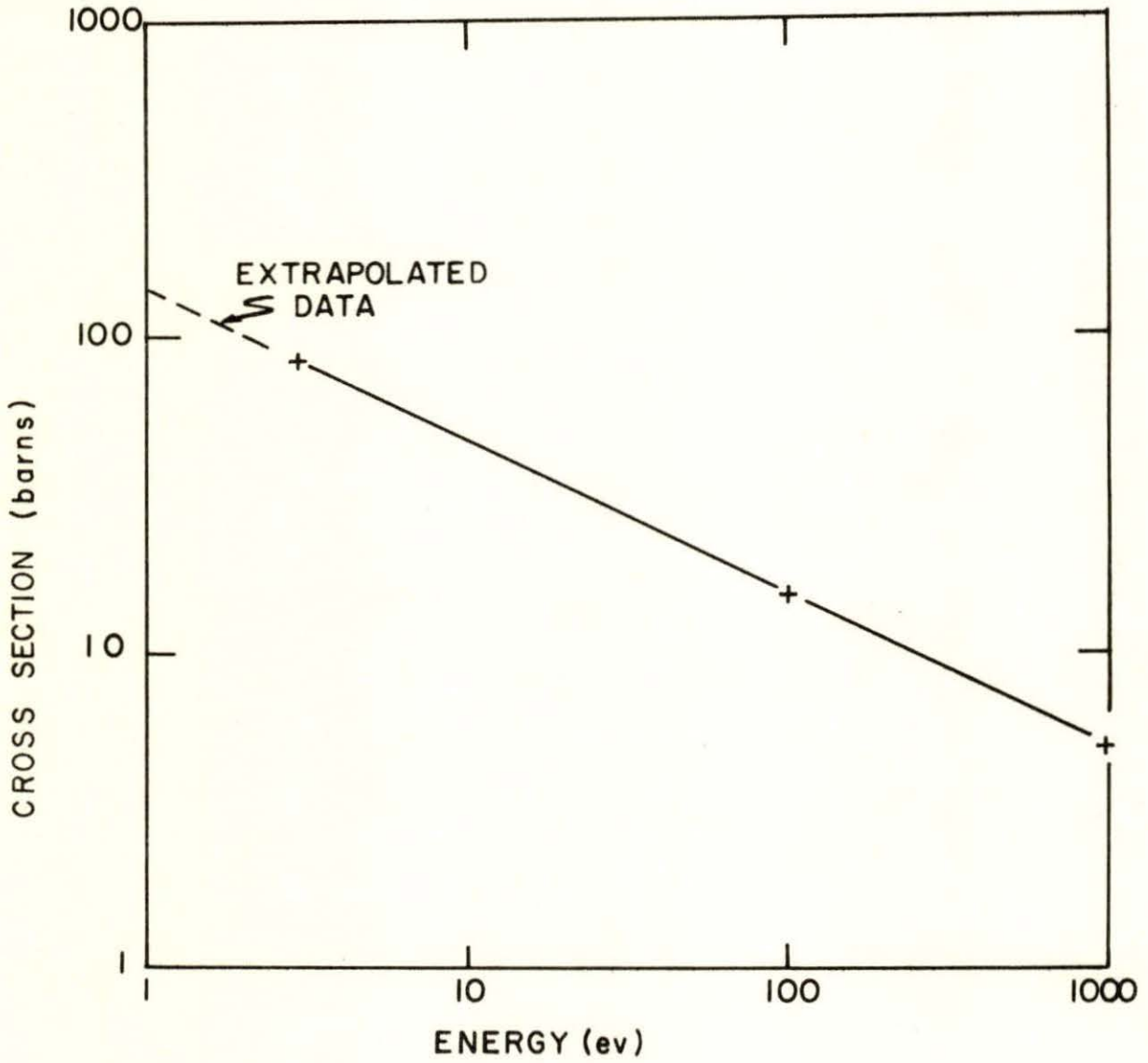


Fig. 3. ${}^6\text{Li}(n, t)$ cross section at low energies.

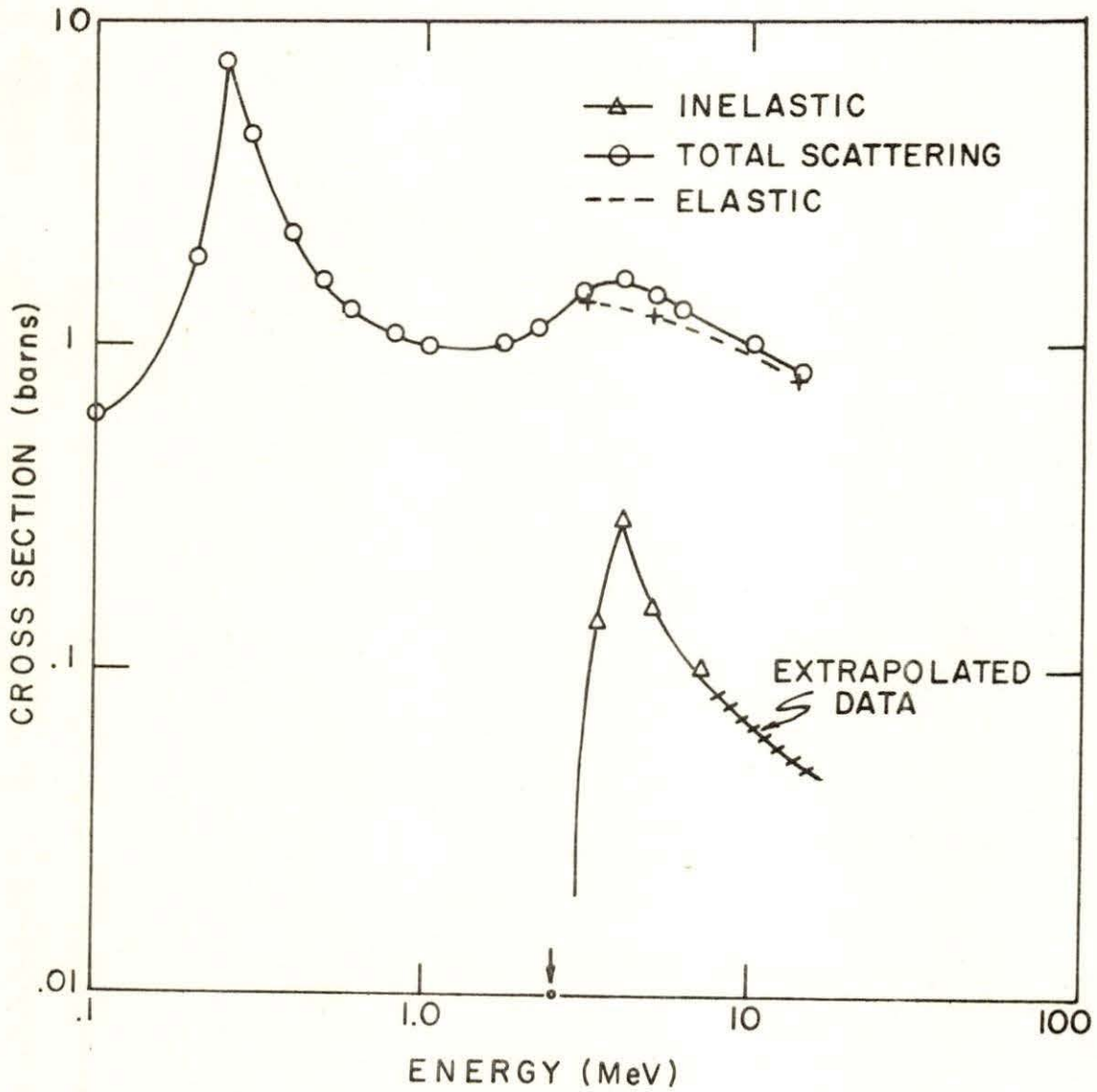


Fig. 4. Li^6 scattering cross sections.

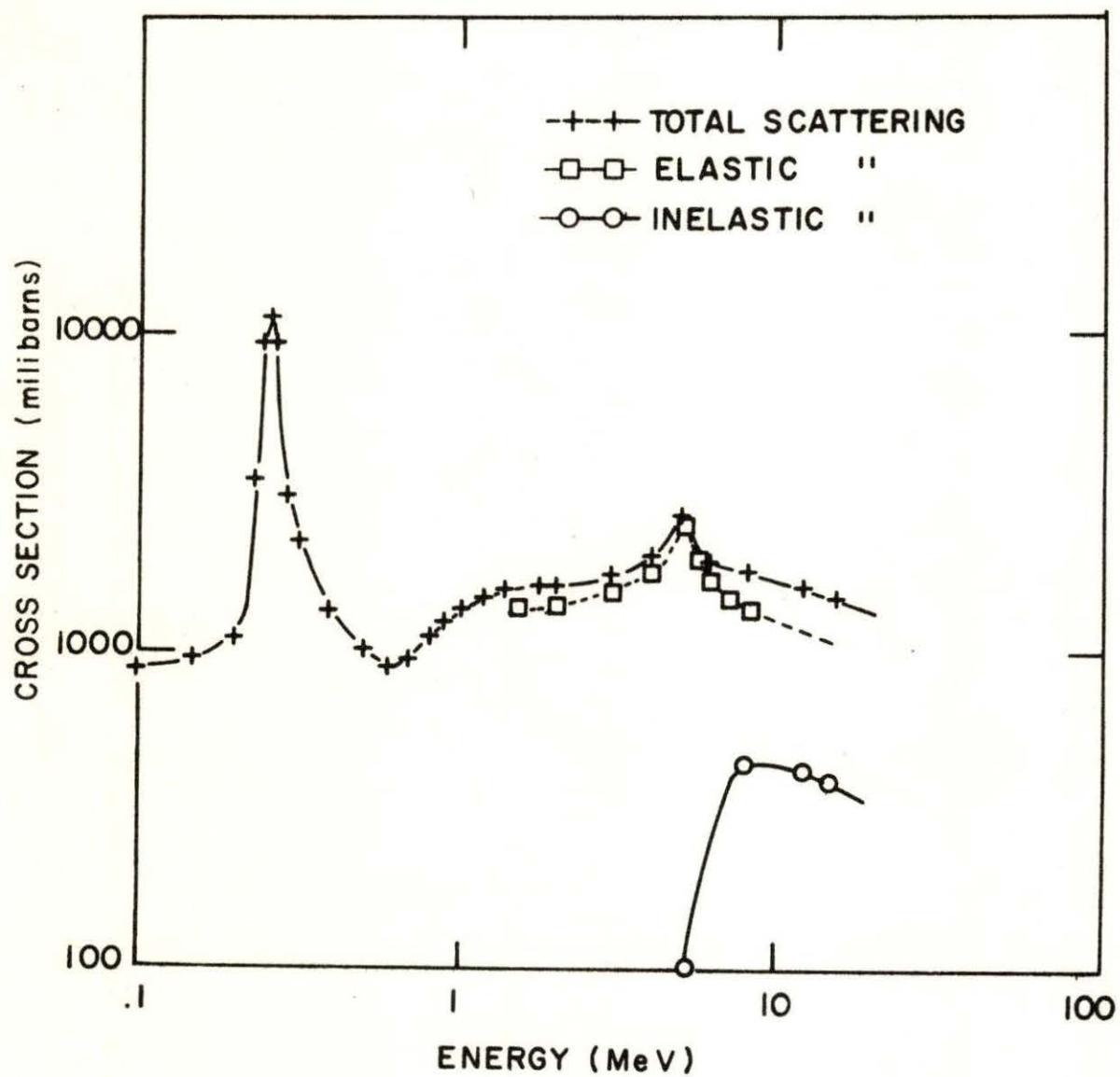


Fig. 5. Li^7 scattering cross sections.

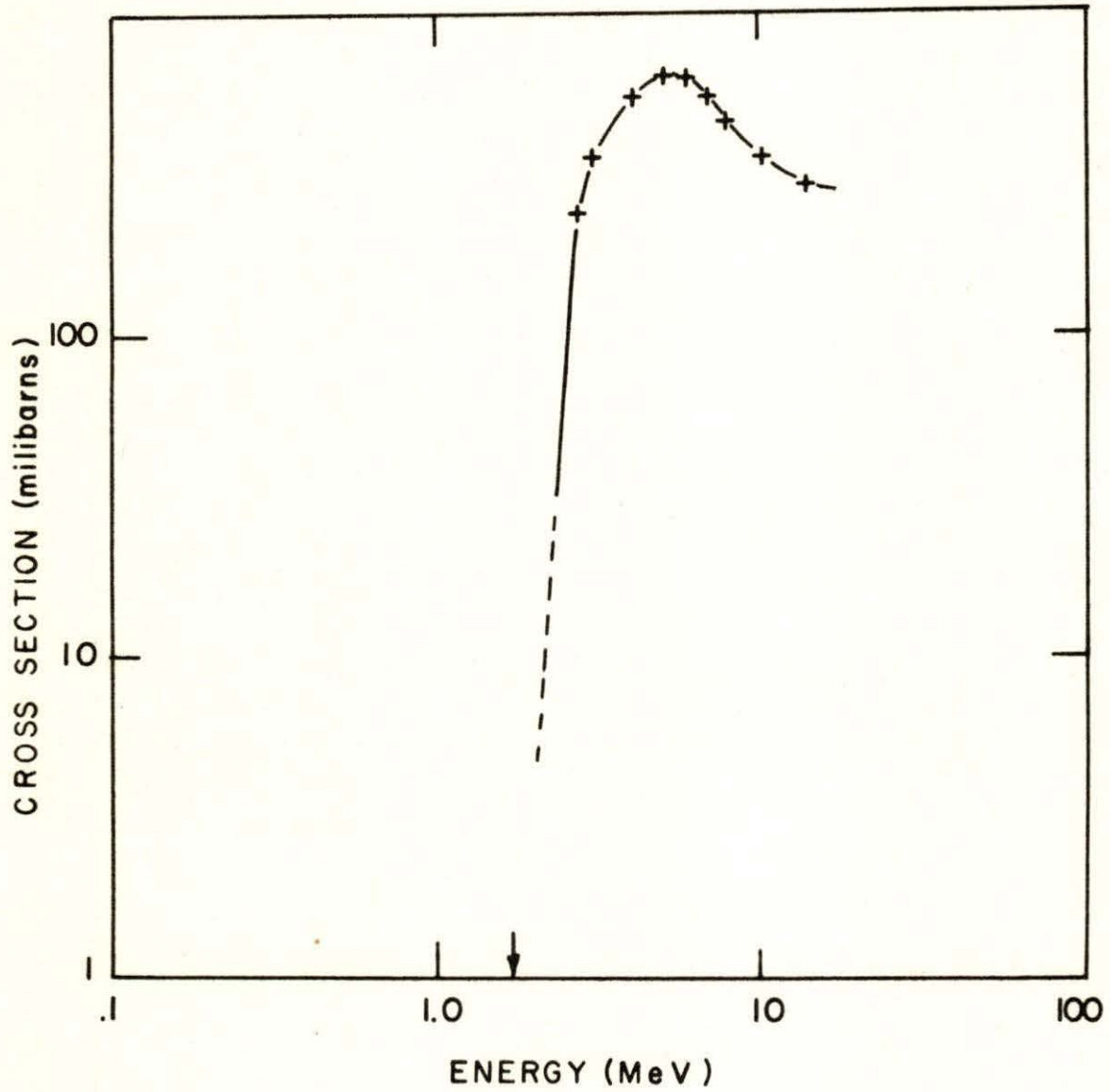


Fig. 6. $\text{Li}^6(n, dn)$ cross section.

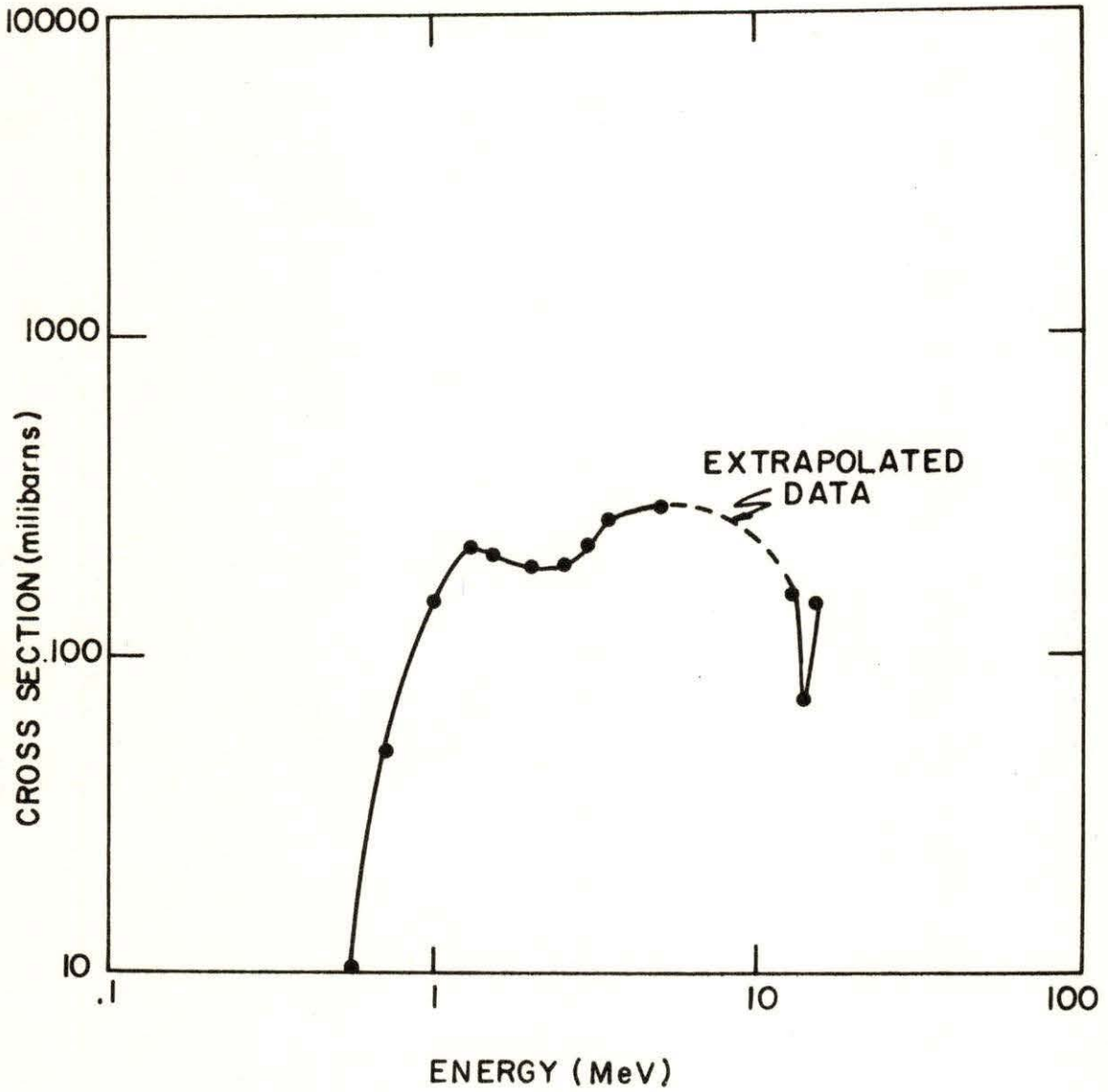


Fig. 7. $\text{Li}^7(n, \gamma)$ cross section (0.478 MeV level).

sections are approximately constant at 0.6 barns and 0.85 barns, respectively. This is common for scattering cross sections of light nuclei such as lithium.

The ${}^6\text{Li}(n, dn)$ reaction and ${}^7\text{Li}(n, tn)$ reaction are interesting in that a neutron is released as a product. The ${}^7\text{Li}(n, tn)$ reaction (see Fig. 2) is endothermic with a Q-value of - 2.47 MeV and, thus, a threshold energy of 2.82 MeV. The ${}^6\text{Li}(n, dn)$ reaction (see Fig. 6) is also endothermic with a Q-value of - 1.47 MeV and a threshold energy of 1.72 MeV. Both reactions must be treated in a special way, since these reactions resemble inelastic scattering rather than absorption or elastic scattering. Each of these reactions involve a three body problem. In the center of mass system, unlike the elastic, two body problem, the resulting products do not have a unique energy and momentum [8]. In particular, the neutron produced by such a reaction can have a spectrum of energies ranging from zero to a maximum energy, which is determined by the individual masses of the products. For example, the three products of the ${}^7\text{Li}(n, tn)$ reaction are tritium, helium, and a neutron (see Fig. 8). The maximum energy that the neutron can have is when the tritium nucleus has zero energy and momentum, and the helium nucleus conserves momentum with the product neutron. If E_L is the total energy in the laboratory system, considering the ${}^7\text{Li}$ atom at rest, the total energy available in the center of mass system is

$$E_c \approx \frac{A}{A+1} E_L = \frac{7}{8} E_L .$$

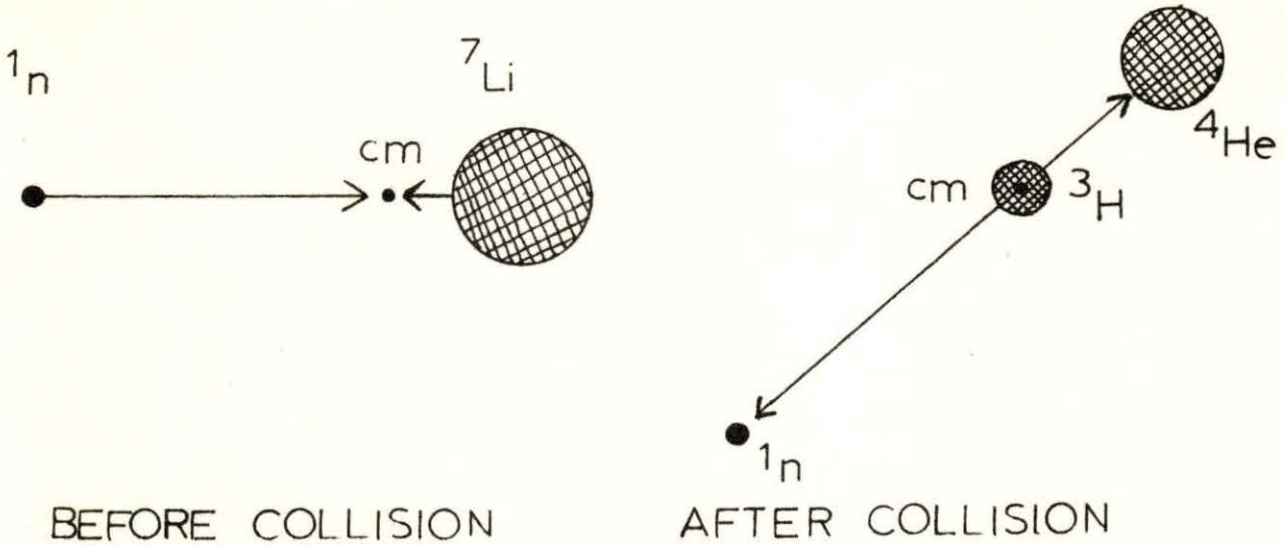


Fig. 8. Maximum neutron energy in the ${}^7\text{Li}(n, tn)$ reaction.

The energy available for motion of the products is $E_c - Q = \frac{7}{8} E_L - Q$ where Q is the Q -value of the reaction. Since this reaction is endothermic, it only occurs at high energies. As a round number, let $E_L = 10$ MeV. The energy available for motion of the particle is then

$$\frac{7}{8} E_L - Q \approx \frac{7}{8} (10) - 2.5 \text{ MeV} \approx 6.25 \text{ MeV.}$$

Using conservation of momentum and energy,

$$M_n V_n = M_{\text{He}} V_{\text{He}},$$

and

$$\frac{1}{2} M_n V_n^2 + \frac{1}{2} M_{\text{He}} V_{\text{He}}^2 = 6.25 \text{ MeV,} \quad (13)$$

where M_n , V_n , M_{He} , and V_{He} are the masses and velocities of the neutron and helium nucleus in the center of mass system, respectively.

Thus, from conservation of momentum

$$V_{\text{He}} = \frac{M_n V_n}{M_{\text{He}}} \approx \frac{V_n}{4},$$

and

$$V_{\text{He}}^2 \approx \frac{V_n^2}{16}.$$

Substituting V_{He}^2 into Eq. (13) and using $M_n \approx 1$ and $M_{\text{He}} \approx 4$,

$$\frac{1}{2} V_n^2 + \frac{1}{8} V_n^2 = 6.25.$$

Thus, the neutron has $\frac{1/2}{1/2 + 1/8} = 4/5$ the total kinetic energy, or about 5 MeV. Thus, a 10 MeV neutron, which lies in the second group, can be scattered with an energy from 0 to 5 MeV. This means it is possible to scatter into any lower energy group. A similar calculation can be made with the ${}^6\text{Li}(n, dn)$ reaction obtaining similar results.

It can be seen that predicting probabilities and energy spectra of neutrons scattered from each group by the ${}^7\text{Li}(n, tn)$ and the ${}^6\text{Li}(n, dn)$ reactions is almost an impossibility. Therefore, in order to treat the ${}^6\text{Li}(n, dn)$ and the ${}^7\text{Li}(n, tn)$ reactions, a simplifying assumption will be made. It will be assumed, according to calculations in the last example, that the energy spectrum of the scattered neutron is flat and that it extends from zero to the next lowest energy group (see Fig. 9). This assumption will hold for both the ${}^6\text{Li}(n, dn)$ and the ${}^7\text{Li}(n, tn)$ reaction. Thus, a neutron in group i which undergoes a ${}^7\text{Li}(n, tn)$ or ${}^6\text{Li}(n, dn)$ reaction can be scattered into any lower energy group with a probability depending only upon the width of the energy group in question. Thus, the probability of landing in group $i - 1$ would be $\Delta E_{i-1}/E_0$, the probability of scattering

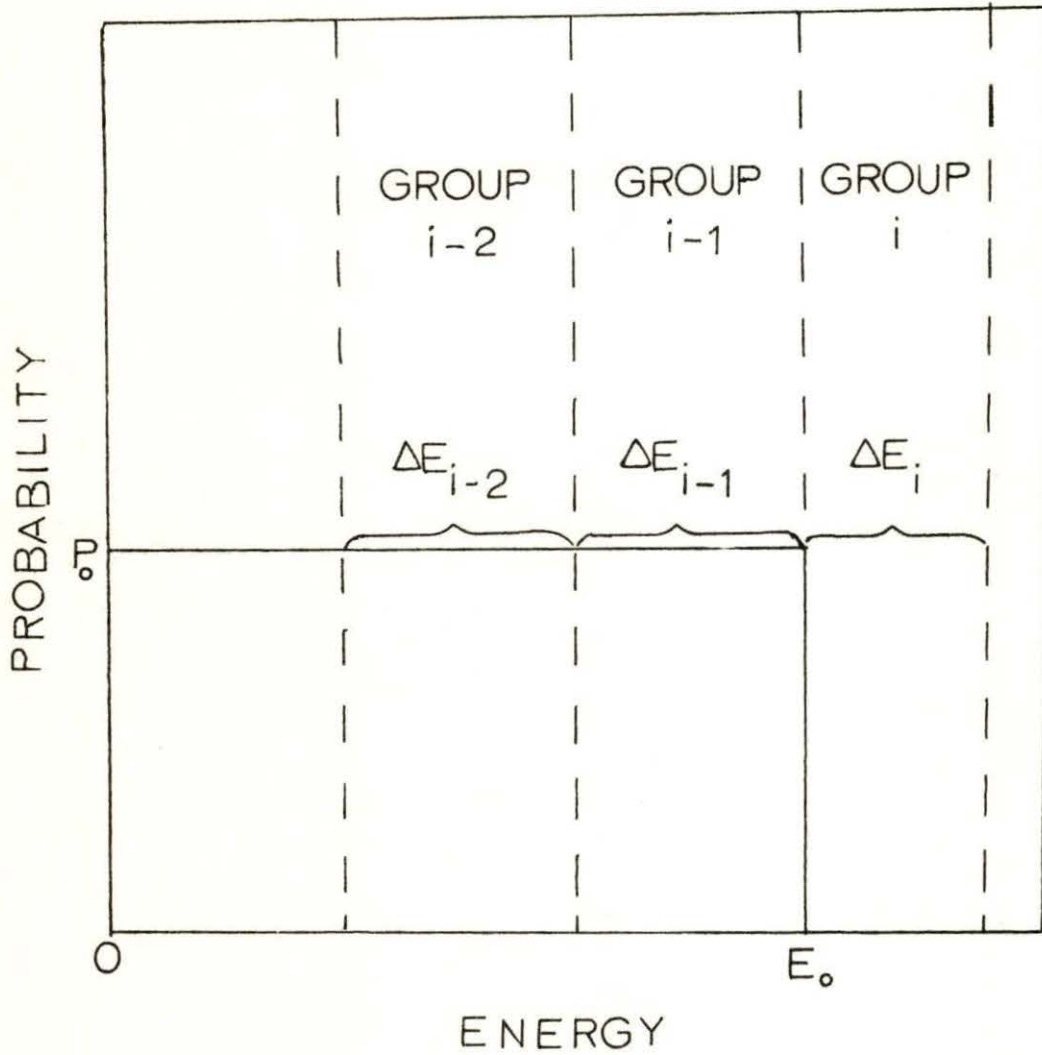


Fig. 9. Probability distribution for the ${}^6\text{Li}(n, dn)$ and ${}^7\text{Li}(n, tn)$ scattering.

into group $i - 2$ would be $\Delta E_{i-2}/E_o$, and so on, where ΔE_{i-1} and ΔE_{i-2} are the energy widths of group $i - 1$ and $i - 2$, respectively. E_o is the lower energy bound of group i . It might be noted that in Fig. 9 the graph is drawn such that

$$\int_0^{E_o} \text{Probability } dE = P_o E_o = 1.$$

Using this criteria, the calculated probabilities are shown in Table I.

A close look at Table I will help justify the assumption that the probability energy distribution is flat for the scattered neutrons from the ${}^7\text{Li}(n, tn)$ reaction and the ${}^6\text{Li}(n, dn)$ reaction. It can be seen that the first groups are much wider compared to the lower energy groups. Therefore, no matter how the probability distribution really looks, a large probability will exist for the neutrons to be scattered into the next few lower energy groups. It should also be pointed out that the ${}^7\text{Li}(n, tn)$ reaction and the ${}^6\text{Li}(n, dn)$ reaction are fairly small compared to the other reactions and occur at high energy ranges. Thus, it is felt that little error will be introduced by incorporating the flat probability distribution into the problem. (Later calculations showed a difference of about 2% in the tritium breeding rates when a slightly different type of distribution was used.)

The ${}^6\text{Li}(n, t)$ reaction and ${}^7\text{Li}(n, \gamma)$ reaction are absorption reactions. The ${}^6\text{Li}(n, t)$ reaction (see Figs. 2 and 3) is exothermic and from thermal energies to approximately 100 Kev has a strong $1/V$ dependence. The Q-value for the ${}^6\text{Li}(n, t)$ reaction is approximately

Table I. Scattering probabilities for the ${}^7\text{Li}(n, tn)$ reaction and the ${}^6\text{Li}(n, dn)$ reaction

Source group (i)	Scatter group (j)	Probability (P^j)
1	2	0.520
1	3	0.274
1	4	0.164
1	5	0.0342
1	6	0.00678
1	7	0.0
1	8	0.0
1	9	0.0
1	10	0.0
2	3	0.571
2	4	0.343
2	5	0.0714
2	6	0.0141
2	7	0.0
2	8	0.0
2	9	0.0
2	10	0.0
3	4	0.800
3	5	0.167
3	6	0.033
3	7	0.0
3	8	0.0
3	9	0.0
3	10	0.0
4	5	0.833
4	6	0.165
4	7	0.0165
4	8	0.0
4	9	0.0
4	10	0.0

8.54 MeV. The ${}^7\text{Li}(n, \gamma)$ reaction is also exothermic and has a Q-value of approximately 2.03 MeV [10].

Of course, the most important reactions are the ${}^6\text{Li}(n, t)$ reaction and the ${}^7\text{Li}(n, tn)$ reaction. These are the only types of reactions

that occur in lithium which yield tritium as a product. It is these reactions that will be used later to calculate the tritium breeding rates in the lithium slabs.

Table II illustrates the different lithium reactions considered in this work and how they are used throughout.

Table II. ${}^6\text{Li}$ and ${}^7\text{Li}$ reactions

Isotope	Reaction	Type and description	Q-value (MeV)	E^{th} (MeV)
${}^6\text{Li}$	(n, t)	Exothermic absorption	+ 8.54	-
${}^6\text{Li}$	Total scattering	Elastic scattering	-	-
${}^6\text{Li}$	(n, dn)	Endothermic inelastic scattering	- 1.47	1.72
${}^7\text{Li}$	(n, tn)	Endothermic inelastic scattering	- 2.47	2.82
${}^7\text{Li}$	(n, γ)	Exothermic absorption	+ 2.03	-
${}^7\text{Li}$	Total scattering	Elastic scattering	-	-

In order to calculate the group microscopic cross sections, the groups have to be determined. The main criterion in the selection of the groups was that all groups were to be directly coupled. Thus, all group energy widths in terms of lethargy had to be greater than $\ln(\frac{1}{\alpha})$. When α was calculated for ${}^6\text{Li}$ and ${}^7\text{Li}$, the following values were obtained:

$$\alpha_6 = 0.509, \text{ and}$$

$$\alpha_7 = 0.562.$$

Thus, for ${}^6\text{Li}$, $\ln \frac{1}{\alpha_6} = 0.675$, and for ${}^7\text{Li}$, $\ln \frac{1}{\alpha_7} = 0.576$. It can be seen that ${}^6\text{Li}$ puts a more stringent requirement on the group lethargy widths. This is to be expected since ${}^6\text{Li}$ is a lighter isotope than ${}^7\text{Li}$, and therefore, more energy can be lost in a single scattering encounter. If the group boundaries are picked such that their lethargy widths are greater than 0.675, each group will be directly coupled, regardless of different isotopic contents of the lithium.

A second major factor in the selection of energy groups was the resonances in the microscopic cross sectional data. In the case of the ${}^6\text{Li}(n, t)$ reaction, ${}^6\text{Li}$ total scattering, and ${}^7\text{Li}$ total scattering, a large resonance occurs at about 0.25 MeV (see Figs. 2, 4, and 5). For this reason, a group was chosen from 0.10 to 0.60 MeV, including these resonances in one group. A small resonance also appears in the ${}^7\text{Li}$ microscopic scattering at about 5 MeV (see Fig. 5). A group from 3 to 7 MeV was chosen to include this resonance. It might be noted that the lethargy width in each case is larger than 0.675.

Since the first, or highest energy group, does not have any neutrons scattered into it from a higher source, group number one does not have to obey the criterion for directly coupled groups. Therefore, group number one was chosen to include the energy interval 14.6 MeV to 15.0 MeV. The reason for this is that in the fusion process 14.8 MeV neutrons are liberated. These neutrons impinge upon the lithium blanket. Thus, a reasonable inner boundary condition for the diffusion

equation would be a constant flux of 14.8 MeV. In the group diffusion method, however, fluxes of one single energy are not calculated.

Rather, fluxes of energy groups are calculated. Thus, the appropriate inner boundary condition would be:

$$\phi^i(0) = \begin{cases} \text{constant} > 0 & \text{for } i = 1 \\ 0 & \text{for } i > 1 \end{cases} .$$

It can be seen, then, that a flux of 14.8 MeV neutrons can best be approximated by a very narrow group centered about 14.8 MeV.

Table III illustrates how the groups were chosen. It might be noted that

$$L^i = \ln \frac{E_u^i}{E_l^i} ,$$

where L^i is the lethargy width of group i and E_u^i and E_l^i are the upper and lower energy bounds of group i , respectively.

After the groups have been determined, microscopic cross sections have to be calculated for each group. The flux as a function of energy is a very complicated function when absorption is present. To facilitate the calculations, the flux as a function of energy is assumed to be constant over each group. Thus,

$$\begin{aligned} \sigma^i &= \frac{\int_i \sigma(E) \phi(E) dE}{\int_i \phi(E) dE} , \\ \text{or} \\ \sigma^i &= \frac{\int_i \sigma(E) dE}{\Delta E_i} , \end{aligned} \tag{14}$$

where $\phi(E)$ is a constant, and ΔE_i is the group energy width. To justify the assumption that $\phi(E)$ is constant, two things must be

Table III. Energy groups and their lethargy widths

Group	Upper energy bound	Lower energy bound	Lethargy width (L^1)
1	15.0 MeV	14.6 MeV	0.0275
2	14.6 MeV	7.0 MeV	0.735
3	7.0 MeV	3.0 MeV	0.847
4	3.0 MeV	0.6 MeV	1.61
5	0.6 MeV	0.1 MeV	1.79
6	0.1 MeV	0.01 MeV	2.31
7	10.0 Kev	1.0 Kev	2.31
8	1.0 Kev	100 ev	2.31
9	100.0 ev	1.0 ev	4.61
10	Thermal		-

remembered. First, the flux need be only considered constant with respect to energy over one group at a time, and not the whole energy width of 14.8 MeV. The value of the constant can be different for each group. It can be seen then that this approximation is very good for narrow groups such as the lower energy groups in Table III.

Secondly, it should be noted that all cross sections, except for the ${}^6\text{Li}(n, t)$ cross section, vary little within each group. Thus, if the cross section is fairly constant within each group, the flux has little effect upon the group cross section. This can be seen in the following.

$$\begin{aligned}\sigma^i &= \frac{\int_i \sigma(E) \phi(E) dE}{\int_i \phi(E) dE}, \\ &\approx \frac{\sigma_o \int_i \phi(E) dE}{\int_i \phi(E) dE}, \\ &\approx \sigma_o,\end{aligned}$$

where the microscopic cross section σ_o is assumed to be constant over group i and is taken out of the integral in the numerator.

The group microscopic cross sections are calculated in the following way. It can be seen that the numerator in Eq. (14) is simply the area under the cross sectional curve determined by the upper and lower energy bounds of group i . Thus, by dividing each group up into small intervals and estimating the cross section in each division, the area under the cross sectional curve in group i can be calculated. By dividing this area by the energy width of group i , an arithmetic average microscopic cross section in each group can be determined. In Table IV is illustrated the results of the microscopic cross sectional calculations.

B. Group Macroscopic Cross Sections

From the group microscopic cross sections, the macroscopic cross sections to be used in the diffusion equation can be calculated. Since the problem necessitates calculations of macroscopic data

Table IV. Group microscopic cross sections

Group	(Barns) ${}^6\text{Li}(n, t)$	(Barns) ${}^7\text{Li}(n, tn)$	(Barns) ${}^6\text{Li}$ scattering	(Barns) ${}^7\text{Li}$ scattering	(Barns) ${}^6\text{Li}(n, dn)$	(Barns) ${}^7\text{Li}(n, \gamma)$
1	0.0275	0.315	0.82	1.45	0.290	0.120
2	0.0409	0.405	1.02	1.72	0.381	0.190
3	0.0905	0.175	1.41	2.06	0.568	0.273
4	0.287	0.0	1.12	1.51	0.0525	0.174
5	1.138	0.0	2.38	1.95	0.0	0.0
6	0.948	0.0	0.600	0.850	0.0	0.0
7	2.59	0.0	0.600	0.850	0.0	0.0
8	7.35	0.0	0.600	0.850	0.0	0.0
9	27.2	0.0	0.600	0.850	0.0	0.0
10	845	0.0	0.600	0.850	0.0	0.0

with differing atom densities of ${}^6\text{Li}$ and ${}^7\text{Li}$, it is convenient to define an independent variable

$$R = \frac{N_6}{N_7},$$

which is simply the atom density ratio of ${}^6\text{Li}$ to ${}^7\text{Li}$. The macroscopic cross sections are then $\Sigma^i = N_7(\sigma_7^i + R\sigma_6^i)$. Using a constant value of N_7 and specifying a value of R , the macroscopic cross sections used in the group diffusion equations can be easily calculated. It might be mentioned at this point that another important independent variable y , which is defined as the atom percent of ${}^6\text{Li}$, can be calculated from R since

$$y = \frac{N_6(100)}{N_6 + N_7} = \frac{R(100)}{R + 1}.$$

The ${}^6\text{Li}(n, t)$ reaction and the ${}^7\text{Li}(n, \gamma)$ reaction are the microscopic absorption cross sections. The macroscopic absorption cross sections can be calculated for group i by

$$\Sigma_a^i = N_7(\sigma_{n\gamma}^i + R\sigma_{nt}^i), \quad (15)$$

where $\sigma_{n\gamma}^i$ represents the ${}^7\text{Li}(n, \gamma)$ microscopic cross section and σ_{nt}^i represents the ${}^6\text{Li}(n, t)$ microscopic cross section for group i .

Similarly, the ${}^6\text{Li}$ and ${}^7\text{Li}$ total microscopic scattering cross sections can be used to obtain the total macroscopic scattering cross section.

Thus, for group i

$$\Sigma_s^i = N_7(\sigma_{s7}^i + R\sigma_{s6}^i), \quad (16)$$

where σ_{s7}^i and σ_{s6}^i are the total microscopic scattering cross sections for ${}^7\text{Li}$ and ${}^6\text{Li}$, respectively.

In order to calculate the transfer coefficients, $\bar{\xi}^i$ must first be calculated. This can be done as follows.

$$\bar{\xi}^i = \frac{\xi_6 \Sigma_{s6}^i + \xi_7 \Sigma_{s7}^i}{\Sigma_s^i}, \quad (17)$$

where ξ_6 and ξ_7 are the average logarithmic energy decrements for ${}^6\text{Li}$ and ${}^7\text{Li}$, respectively,

$$\Sigma_{s6}^i = N_6 \sigma_{s6}^i,$$

and

$$\Sigma_{s7}^i = N_7 \sigma_{s7}^i.$$

Thus,

$$\bar{\xi}^i = \frac{\xi_6 N_6 \sigma_{s6}^i + \xi_7 N_7 \sigma_{s7}^i}{N_7 (\sigma_{s7}^i + R \sigma_{s6}^i)},$$

or

$$\bar{\xi}^i = \frac{\xi_6 R \sigma_{s6}^i + \xi_7 \sigma_{s7}^i}{\sigma_{s7}^i + R \sigma_{s6}^i}.$$

ξ_6 and ξ_7 were calculated to be

$$\xi_6 = 0.295, \text{ and}$$

$$\xi_7 = 0.254.$$

Thus,

$$\bar{\xi}^i = \frac{0.295 R \sigma_{s6}^i + 0.254 \sigma_{s7}^i}{\sigma_{s7}^i + R \sigma_{s6}^i}. \quad (18)$$

The macroscopic transfer coefficients are now ready to be calculated. It might be remembered that all groups are directly coupled,

and thus, neutrons which are elastically scattered from the ${}^6\text{Li}$ and ${}^7\text{Li}$ total scattering cross sections enter only the group directly below. Neutrons that are inelastically scattered due to the ${}^7\text{Li}(n, \text{tn})$ and the ${}^6\text{Li}(n, \text{dn})$ reactions are able to scatter into several lower energy groups. Thus,

$$\begin{aligned}\Sigma_s(i \rightarrow i+1) &= \frac{\bar{\Sigma}_s^i}{L^i} + [N_7 \sigma_{\text{ntn}}^i + N_6 \sigma_{\text{ndn}}^i] P^{i+1}, \\ &= \frac{\bar{\Sigma}_s^i}{L^i} + N_7 P^{i+1} (\sigma_{\text{ntn}}^i + R \sigma_{\text{ndn}}^i),\end{aligned}\quad (19)$$

where L^i is the group lethargy width (see Table III), $\bar{\Sigma}_s^i$ is the group lethargy decrement (see Eq. (18)), Σ_s^i is the total macroscopic scattering cross section (see Eq. (16)), P^{i+1} is the probability of scattering into group $i+1$ due to the ${}^7\text{Li}(n, \text{tn})$ reaction and the ${}^6\text{Li}(n, \text{dn})$ reaction (see Table I), σ_{ntn}^i is the microscopic cross section for the ${}^7\text{Li}(n, \text{tn})$ reaction, and σ_{ndn}^i is the microscopic cross section for the ${}^6\text{Li}(n, \text{dn})$ reaction. For scattering into energy groups lower than $i+1$,

$$\Sigma_s(i \rightarrow j) = N_7 P^j (\sigma_{\text{ntn}}^i + R \sigma_{\text{ndn}}^i) \quad (20)$$

for $j > i+1$, and P^j is the probability of the neutron landing in group j . In Eq. (19) the first term represents the neutrons that are scattered into group $i+1$ from group i due to elastic scattering, while the second term represents neutrons scattered into group $i+1$ from group i due to the ${}^7\text{Li}(n, \text{tn})$ reaction and the ${}^6\text{Li}(n, \text{dn})$ reaction. Since the groups are directly coupled by elastic scattering, only the neutrons from the ${}^6\text{Li}(n, \text{dn})$ reaction and the ${}^7\text{Li}(n, \text{tn})$

reaction can be scattered into groups lower than $i + 1$, as is shown by Eq. (20).

Using Eqs. (15), (16), (18), (19), and (20), all macroscopic cross sections for a specific value of R can be calculated for use in the group diffusion equation.

C. Diffusion Coefficients

From Fick's Law the diffusion coefficient is defined as

$$D = \frac{\Sigma_s}{3\Sigma_t^2},$$

where Σ_s is the macroscopic scattering cross section and Σ_t is the total macroscopic cross section. In deriving the equation, however, it was assumed that the scattering was isotropic in the lab system and that there was little absorption. Neither of these assumptions hold in this problem.

It is possible, however, to compensate for moderate anisotropic scattering by using transport corrections to the diffusion coefficients. From methods of transport theory it is found that

$$\frac{\Sigma_s}{2} \sqrt{\frac{D}{\Sigma_a}} \ln \left[\frac{\Sigma_t + \sqrt{\frac{\Sigma_a}{D}}}{\Sigma_t - \sqrt{\frac{\Sigma_a}{D}}} \right] = \frac{1 + 3D\Sigma_s \bar{u}}{1 + 3D\Sigma_t \bar{u}},$$

where \bar{u} is the average value of the cosine of the scattering angle in the lab system. An approximation of this equation can be obtained by expanding the logarithm in a series of powers of Σ_a/Σ_t . The result is

$$\Sigma_a/D = 3(\Sigma_a + \Sigma_s)\Sigma_a \left(1 - \frac{4}{5} \frac{\Sigma_a}{\Sigma_a + \Sigma_s}\right)$$

(see reference [7], p. 127).

Since the diffusion coefficient is going to be different for each energy group,

$$\frac{\Sigma_a^i}{D^i} = 3(\Sigma_a^i + \Sigma_s^i)\Sigma_a^i \left(1 - \frac{4}{5} \frac{\Sigma_a^i}{\Sigma_a^i + \Sigma_s^i}\right). \quad (21)$$

Here Σ_a^i is chosen so that

$$\Sigma_a^i = N_7\sigma_{n\gamma}^i + N_6\sigma_{nt}^i + N_7\sigma_{ntn}^i + N_6\sigma_{ndn}^i,$$

or

$$\Sigma_a^i = N_7(\sigma_{n\gamma}^i + \sigma_{ntn}^i + R\sigma_{nt}^i + R\sigma_{ndn}^i), \quad (22)$$

where N_7 , $\sigma_{n\gamma}^i$, σ_{nt}^i , σ_{ntn}^i , σ_{ndn}^i , and R are defined as before. Σ_s^i is calculated from Eq. (16). Using Eqs. (22) and (16) and substituting into Eq. (21), all diffusion coefficients for each group and for a specific value of R can be calculated.

The first results of the fluxes and integrated fluxes calculated from FAIMOS indicated that the calculations needed to be somewhat refined. This could be seen by a close look at the flux of group 1. The flux of group 1 should represent a purely exponential decay, given by

$$\phi^1(r) = e^{-\Sigma_t^1 r}, \quad (23)$$

where Σ_t^1 is the total removal cross section of group 1 and is given by

$$\Sigma_t^1 = \Sigma_a^1 + \sum_{j=2}^{10} \Sigma_s(1 \rightarrow j).$$

In this case $\phi^1(r)$ represents the uncollided flux. For a slab of lithium of width w ,

$$\begin{aligned} \int_0^w \phi^1(r) dr &= \int_0^w e^{-\Sigma_t^1 r} dr, \\ &= \frac{-1}{\Sigma_t^1} e^{-\Sigma_t^1 r} \Big|_0^w. \end{aligned}$$

If w is large,

$$\int_0^w \phi^1(r) dr \approx \frac{1}{\Sigma_t^1}. \quad (24)$$

Thus, by comparing $1/\Sigma_t^1$ with the integrated flux of group 1 calculated by FAIMOS, an indication of the error involved could be seen.

An example of these results is shown in Fig. 10. The calculated first group flux from FAIMOS and the graph of Eq. (23) are shown for $R = 0.2$ and $w = 100$ cm. In this case $\Sigma_t^1 = 0.5914 \text{ cm}^{-1}$, and $\frac{1}{\Sigma_t^1} = 1.69$. It can be seen that the flux calculated by FAIMOS is not in agreement with Eq. (23). The integrated flux of group 1 is 2.95, which is in considerable error with the expected result of 1.69.

This error is due to the inaccuracies of diffusion theory at high energies. It is possible, however, to adjust the diffusion coefficient, D^1 , and somewhat correct for this error. In this example the calculated value of $D^1 = 5.15$ is used to obtain the flux in Fig. 10. When D^1 is adjusted to 1.55, the integrated flux for group 1 is

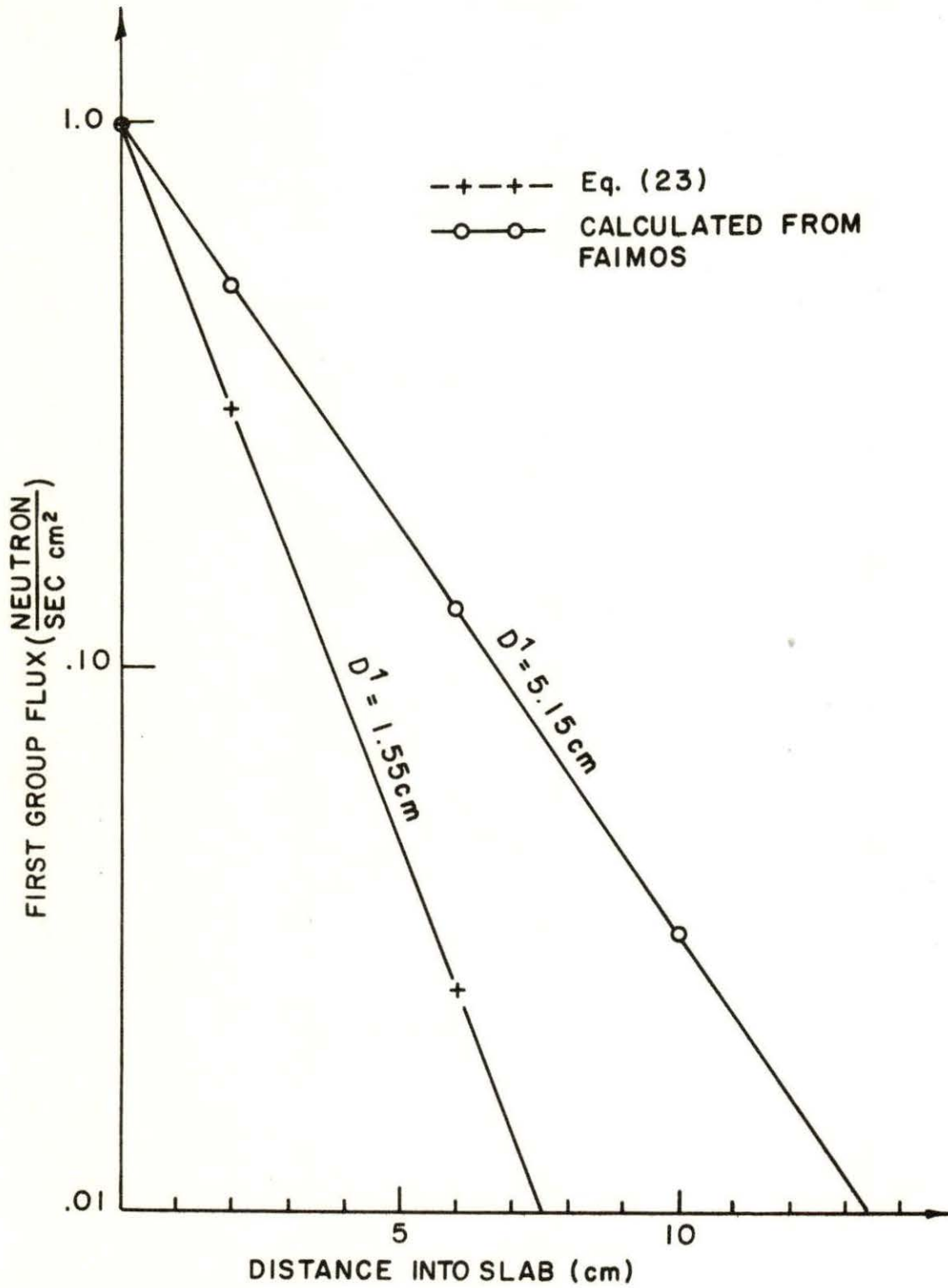


Fig. 10. $\phi^1(r)$ for $R = 0.20$ and $w = 100$ cm.

calculated at 1.694, which is in good agreement with the predicted result (see Fig. 10).

The diffusion coefficient for the first group was adjusted in each case until the integrated flux for group 1 was in fair agreement with $1/\Sigma_t^1$. This was done by a trial and error manner with three or four trials being necessary to adjust D^1 to the proper value. Values for the diffusion coefficients for all other groups are calculated from Eq. (21).

D. Calculations of Constants for the Diffusion Equation

A computer program specifically designed to use Eqs. (15), (16), (18), (19), (20), (21), and (22) was developed to calculate the constants for use in the multi-group diffusion equation. D^i , Σ_a^i , $\bar{\xi}^i$, Σ_s^i and $\Sigma_s(i \rightarrow j)$ were calculated using values of $0 \leq R \leq 9$ in steps of 0.05. A value of $N_7 = 0.0378 \times 10^{+24}$ atoms per cm^3 , which is the atom density of molten lithium at 1300 °F, was used [2]. From the use of this program, all constants and cross sectional data were generated for blankets of 100% ^7Li to 10% ^7Li and 90% ^6Li , or values of $0 \leq y \leq 0.90$. In order to present typical values of group constants used in FAIMOS, representative calculations of Σ_a^i , Σ_s^i , $\bar{\xi}^i$, D^i , and $\Sigma_s(i \rightarrow j)$ are given in Tables V and VI. Similar data were prepared for other values of R.

Table V. Group macroscopic cross sections and constants for $R = 0.25$, or a blanket of 20% ${}^6\text{Li}$ and 80% ${}^7\text{Li}$

Group	Σ_a^i (cm^{-1})	Σ_s^i (cm^{-1})	$\bar{\nu}^i$	D^i (cm)
1	0.0048	0.0626	0.259	5.02
2	0.00757	0.0747	0.259	4.17
3	0.0112	0.0912	0.260	3.48
4	0.00929	0.0677	0.260	4.79
5	0.0108	0.0962	0.264	3.39
6	0.00896	0.0378	0.260	8.42
7	0.0245	0.0378	0.260	7.81
8	0.0695	0.0378	0.260	6.45
9	0.257	0.0378	0.260	3.74
10	7.99	0.0378	0.260	0.204

E. Tritium Breeding Rates

In order to calculate the tritium breeding rate for a specific concentration of ${}^6\text{Li}$ and ${}^7\text{Li}$, the group fluxes must first be calculated. The multi-group diffusion Eq. (5) was used for this purpose. Lithium, however, is not fissionable, and, therefore all χ^i are zero. The multi-group diffusion equation applicable to lithium is then

$$D^i \nabla^2 \phi^i(r) - \Sigma_a^i \phi^i(r) - \sum_{j=i+1}^N (\Sigma_s(i \rightarrow j)) \phi^j(r) + \sum_{j=1}^{i-1} (\Sigma_s(j \rightarrow i)) \phi^j(r) = 0. \quad (25)$$

Table VI. Transfer coefficients for $R = 0.25$ or a blanket of 20% ${}^6\text{Li}$ and 80% ${}^7\text{Li}$

(i) Source group	(j) Receiving group	$\Sigma_s(i \rightarrow j)$ (cm^{-1})
1	2	0.597
1	3	0.00401
1	4	0.0024
1	5	0.000501
1	6	0.000103
2	3	0.0371
2	4	0.00649
2	5	0.00135
2	6	0.00267
3	4	0.0376
3	5	0.0020
3	6	0.00395
4	5	0.0114
4	6	0.0000819
4	7	0.00000819
5	6	0.0142
6	7	0.00426
7	8	0.00426
8	9	0.00426
9	10	0.00213

Since ten groups were chosen, Eq. (25) represents ten simultaneous, linear, second order differential equations in one dimension. Twenty boundary conditions are needed to solve Eq. (25). The ten inner boundary conditions are

$$\phi^i(0) = \begin{cases} 1 & \text{for } i = 1 \\ 0 & \text{for } 1 < i \leq 10 \end{cases} \quad (26)$$

Equation (26) closely represents a flux of one neutron per cm^2 per second at 14.8 MeV incident upon the inner face of the infinite slab. The outer boundary conditions are set so that no return current enters the slab [5], or that

$$\phi^i(w + d^i) = 0, \text{ for } 1 \leq i \leq 10, \quad (27)$$

where w is the thickness of the slab and d^i is the extrapolated boundary for group i . FAIMOS automatically calculates each d^i .

Upon solving Eqs. (25), (26), and (27) simultaneously, unique solutions to ten fluxes as a function of position throughout the lithium slab are computed. The multi-group computer code FAIMOS is used to obtain the solutions to the group fluxes.

The output of FAIMOS gives the values of the ten group fluxes as they vary throughout the lithium blanket. FAIMOS also calculates the integrated fluxes over position, or

$$(\text{IF})^i = \int_0^w \phi^i(r) dr,$$

where $(\text{IF})^i$ is the integrated flux of group i and w is the width of the blanket. The average value of $\phi^i(r)$ through the slab can then be found by

$$\bar{\phi}^i = \frac{\int_0^w \phi^i(r) dr}{w} = \frac{(IF)^i}{w},$$

where $\bar{\phi}^i$ is the average value of $\phi^i(r)$ over the width of the lithium blanket.

From the average group fluxes, the breeding rate resulting from the ${}^7\text{Li}(n, tn)$ reaction can be calculated by,

$$BR_7 = \sum_{i=1}^{10} \Sigma_{ntn}^i \bar{\phi}^i,$$

where $\Sigma_{ntn}^i = N_7 \sigma_{ntn}^i$, and $\Sigma_{ntn}^i \bar{\phi}^i$ is the breeding rate in group i .

The breeding rate resulting from the ${}^6\text{Li}(n, t)$ reaction is

$$BR_6 = \sum_{i=1}^{10} \Sigma_{nt}^i \bar{\phi}^i,$$

where $\Sigma_{nt}^i = N_6 \sigma_{nt}^i$, and $\Sigma_{nt}^i \bar{\phi}^i$ is the breeding rate in group i . The total tritium breeding rate is then

$$\begin{aligned} BR_{\text{total}} &= BR_7 + BR_6, \\ &= \sum_{i=1}^{10} [(\Sigma_{ntn}^i + \Sigma_{nt}^i) \bar{\phi}^i], \\ &= N_7 \sum_{i=1}^{10} [(\sigma_{ntn}^i + R \sigma_{nt}^i) \bar{\phi}^i]. \end{aligned} \quad (28)$$

Since Σ_{ntn}^i and Σ_{nt}^i are functions of R and $\bar{\phi}^i$ is a function of R and w , the total tritium breeding rate is also a function of R and w . By setting the width of the blanket as constant and calculating the total tritium breeding rate for different values of R , an optimum breeding rate can be found. A computer program was written that used Eq. (28) to calculate the total tritium breeding rates.

V. DISCUSSION OF RESULTS

The total tritium breeding rates are calculated for different concentrations of ${}^6\text{Li}$ in a 100 cm slab and a 200 cm slab. Figures 13 and 14 show the results of the total tritium breeding rate calculations as a function of concentration of ${}^6\text{Li}$ for both slab widths.

Before discussing Figs. 13 and 14, some interesting results can be obtained by looking at Table VII. In Table VII the ranges in the percentage of the total breeding rate for each group are given for both slab widths. It can be seen that in each slab width, between 80% and 90% of the tritium is bred in groups 1, 2, 3, and 5. The

Table VII. Ranges in the percent of total breeding rates for each group in 100 cm slab and 200 cm slab. Ranges were taken from 0% to 30% ${}^6\text{Li}$

Group	Relative breeding rates for w = 100 cm (%)	Relative breeding rates for w = 200 cm (%)
1	21.0-26.3	29.1-33.9
2	43.4-54.6	38.1-55.1
3	9.5-11.0	8.4-11.0
4	1.2-7.3	0.0-6.4
5	2.8-11.3	0.0-10.0
6	2.0-5.8	0.0-5.3
7	1.5-1.7	0.0-2.3
8	0.3-0.6	0.0-1.2
9	0.0-0.1	0.0-0.3
10	0.0-0.0	0.0-0.0

breeding in groups 1 and 2 is due mostly to the ${}^7\text{Li}(n, tn)$ reaction. In group 5 the breeding is due entirely to ${}^6\text{Li}$, and is the result of the resonance in the ${}^6\text{Li}(n, t)$ cross section at about .26 MeV (see Fig. 2). It can also be seen from Table VII that there is virtually no tritium bred at thermal energies. This surprising result stems from the fact that most of the neutrons are absorbed before becoming thermalized.

It can be concluded, therefore, from Table VII that the choice of groups used in this paper is a somewhat poor one. It can be seen that about 50% of all the tritium breeding occurs in group 2. This, of course, is due to its large energy width which was necessary in order to make all groups directly coupled. For future calculations, it would be advisable to choose the groups so that the energy range from 3 to 15 MeV is split into narrow groups, thus, doing away with directly coupled groups. The lowest energy group could probably be made from 0 to 1.0 MeV since hardly any breeding was done in this energy range.

In Figs. 11 and 12 a representative example of the group fluxes is shown for $R = 0.20$ in the 100 cm slab and the 200 cm slab, respectively. Only groups 1, 2, 3, 4, 5, 6, and 7 are shown since hardly any tritium is bred in the energy ranges below group 7. From Figs. 11 and 12 it can easily be seen why virtually no tritium is bred below group 7 since all fluxes below this are decreased by a factor of 1000 or more. Another conclusion that can be drawn from Fig. 12 is that increasing the width of the slab beyond 100 cm is almost pointless in regard to the total amount of tritium being bred.

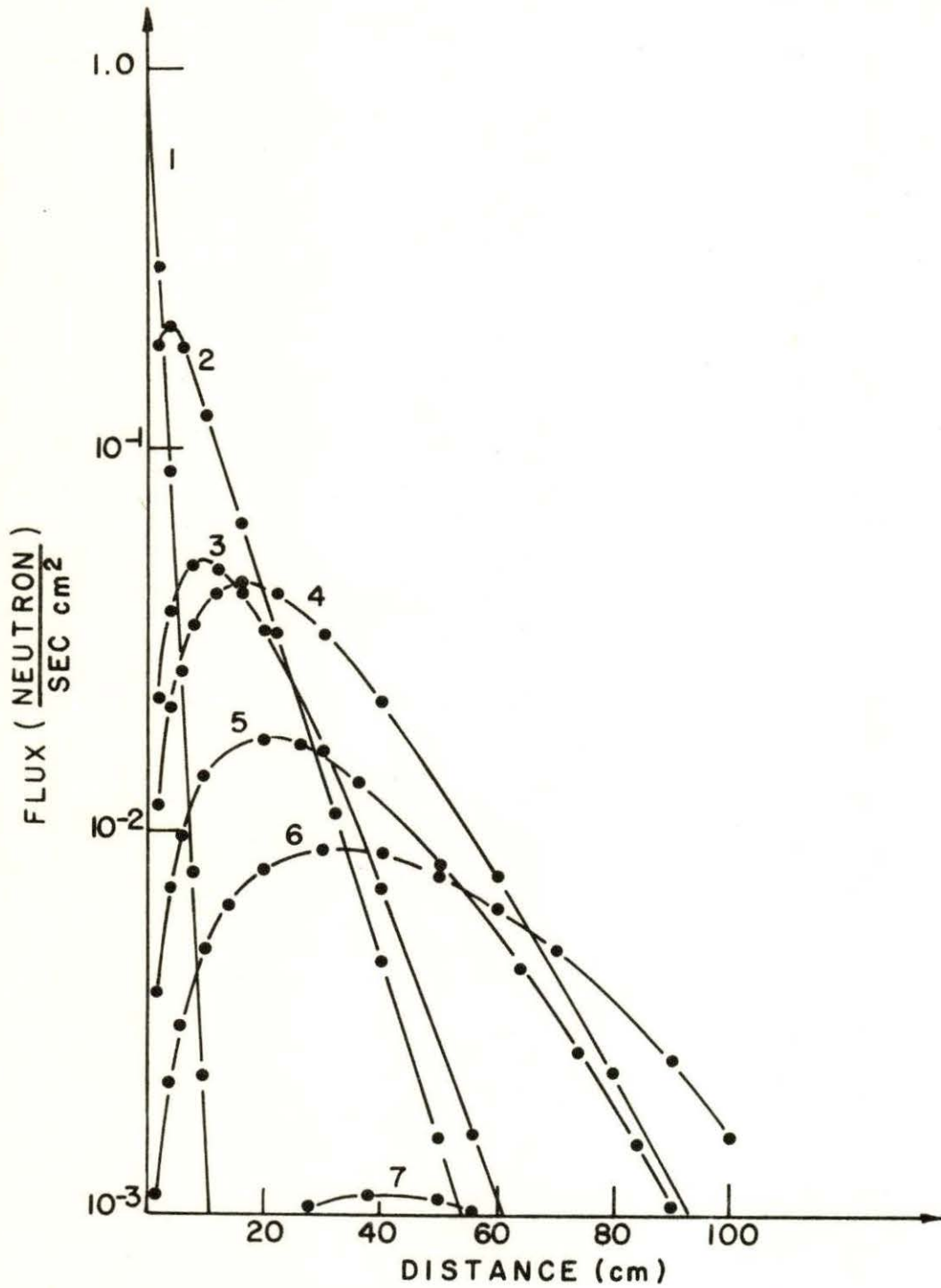


Fig. 11. Fluxes of groups 1-7 for $w = 100$ cm and 16.7% ${}^6\text{Li}$ concentration ($R = 0.20$).

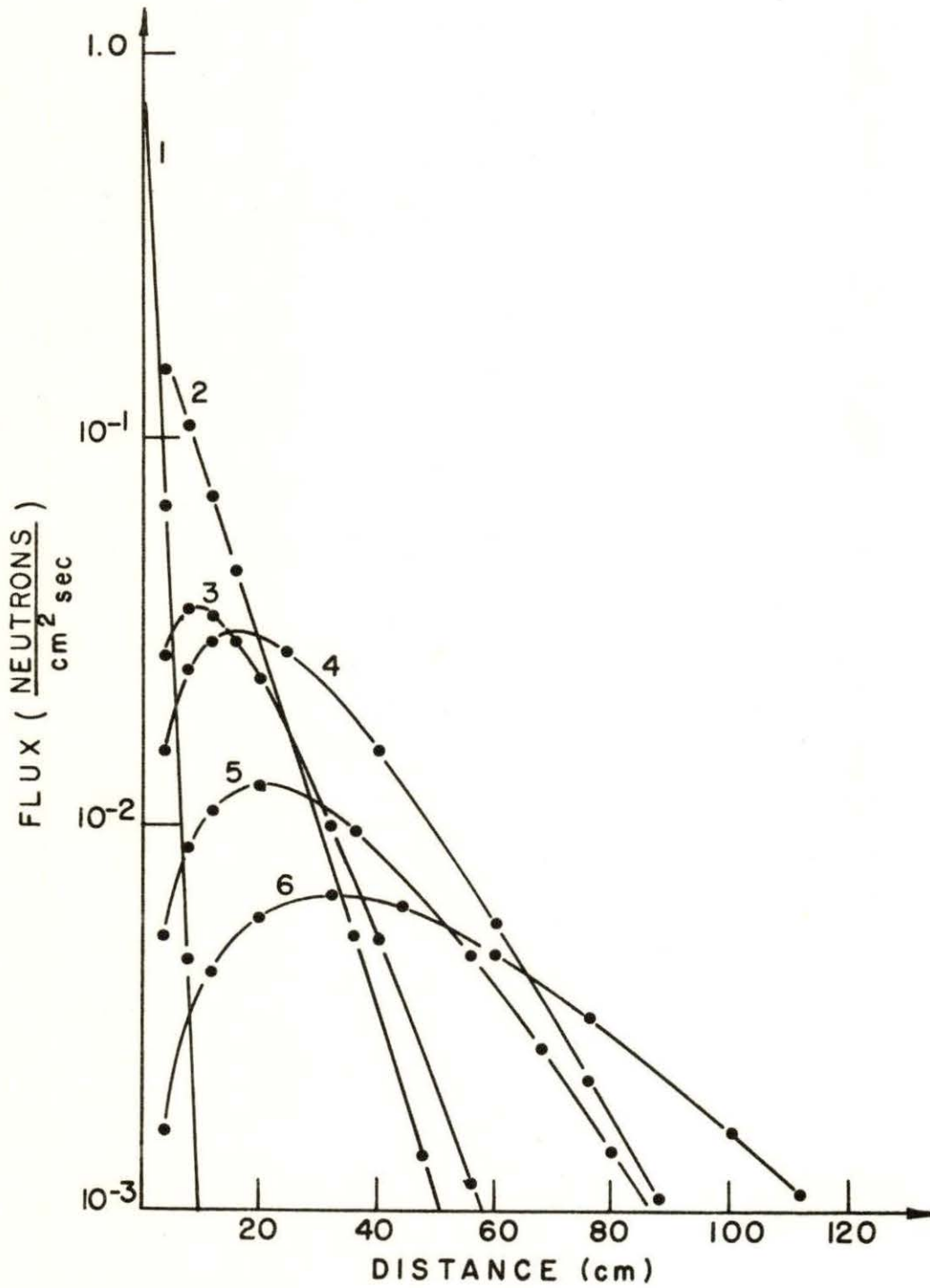


Fig. 12. Fluxes of groups 1-6 for $w = 200$ cm and 16.7% ${}^6\text{Li}$ concentration ($R = 0.20$).

It can be seen that the group fluxes which do the most breeding are decayed to very low values after 120 cm. This would tend to suggest that virtually all the breeding is done in the first 100 cm, and any added thickness beyond this would breed very little more tritium.

One of the first things noticed by comparing Figs. 13 and 14 is the relative heights of the two peaks. In the 100 cm slab the peak is at a value of 0.819×10^{-3} tritons per cm^3 per second, while in the 200 cm slab the peak is at a smaller value of 0.343×10^{-3} tritons per cm^3 per second. No conclusion, however, can be drawn from this result. The reason for this lies in the way in which the fluxes in each of the two widths are normalized. The group fluxes are normalized so that

$$\int_0^w S(r) dr = 1,$$

where

$$S(r) = \sum_{i=1}^{10} \nu \Sigma_f^i \phi^i(r).$$

The same $(\nu \Sigma_f^i)^i$ are used for each slab width and for each ${}^6\text{Li}$ concentration. Using the same $(\nu \Sigma_f^i)^i$ in each ${}^6\text{Li}$ concentration assures that the group fluxes in a single width are normalized equally.

When w is increased from 100 cm to 200 cm, however, the size of the limits of integration on the source are doubled in size. Since the values for $(\nu \Sigma_f^i)^i$ do not change, and since an integrated source of 1 neutron per cm^3 per second is calculated in each width, the group fluxes for the 200 cm slab have to be relatively smaller than the group fluxes in the 100 cm slab. This, of course, results in

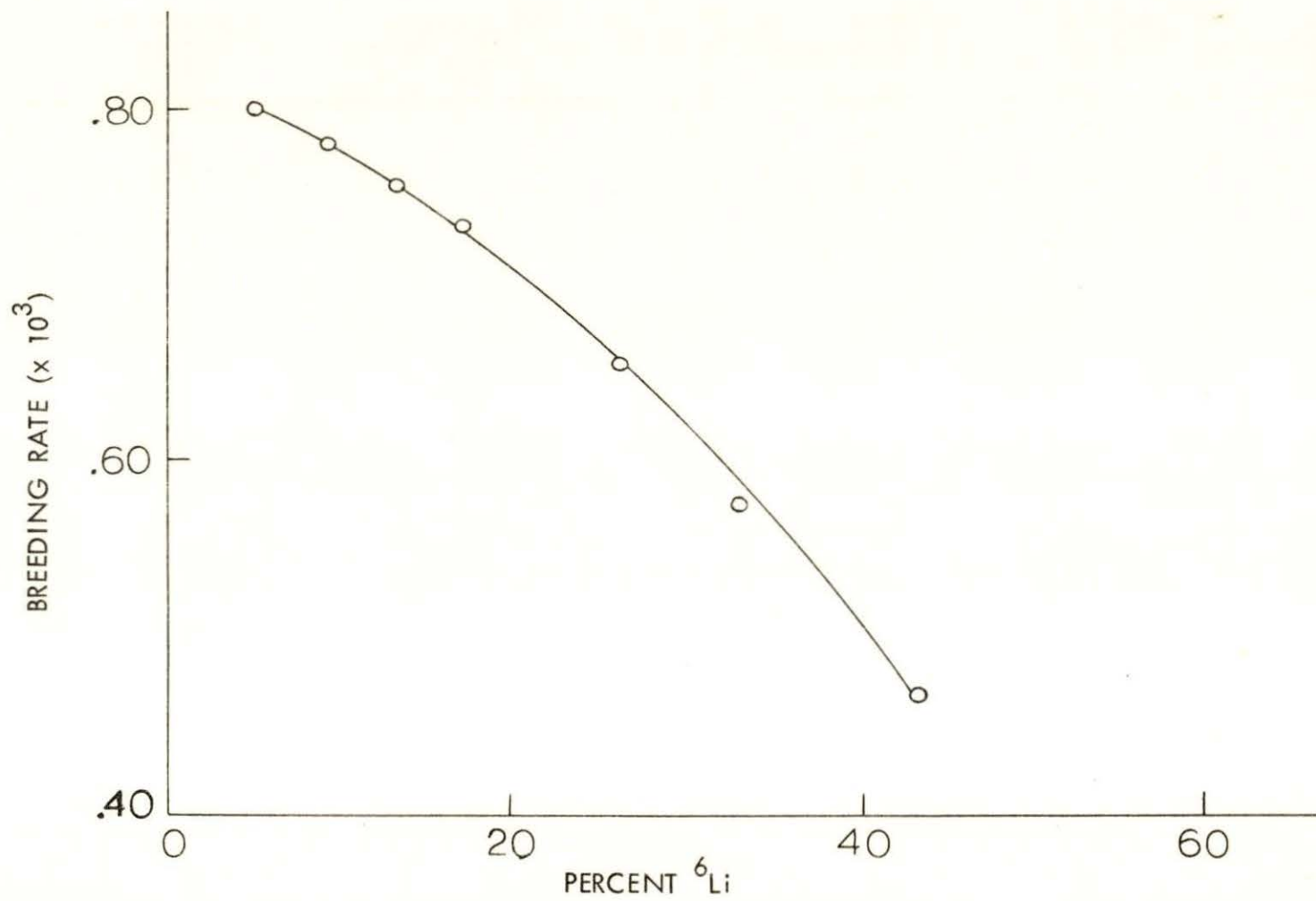


Fig. 13. Total tritium breeding rate for $w = 100$ cm.

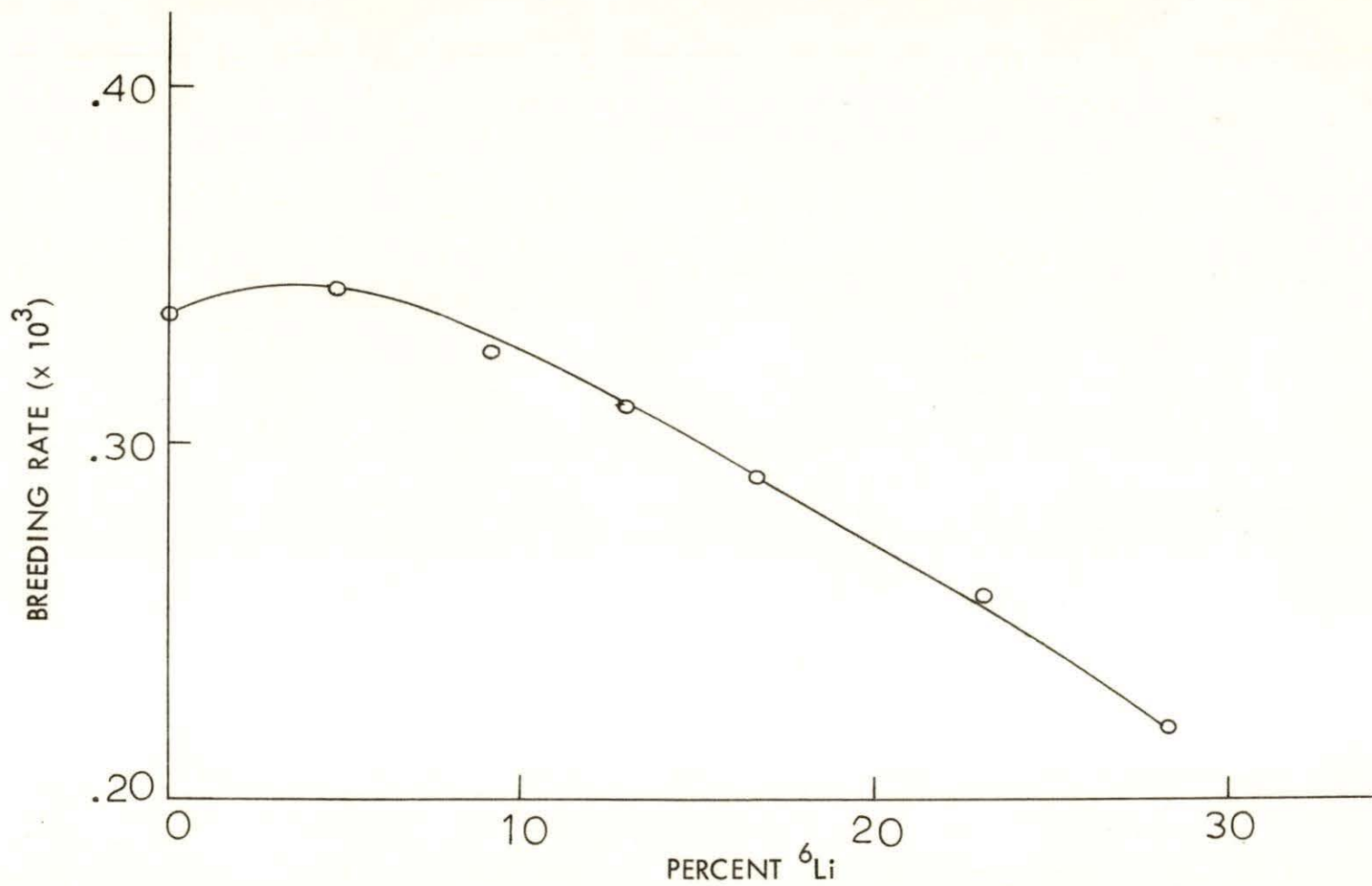


Fig. 14. Total tritium breeding rate for $w = 200$ cm.

lower breeding rates for the 200 cm slab. It might also be pointed out that the relationship between increasing the integration limits and, thereby, decreasing the group fluxes is not linear. In other words, the breeding rates in the 200 cm slab cannot be doubled and then compared with the breeding rates in the 100 cm slab. It would be logical, however, to expect a slightly greater breeding rate in the 200 cm slab since the leakage would be less. Also, more lithium is available for tritium production in the larger slab.

In Figs. 13 and 14 the position of the optimum tritium breeding rate occurs at 5% ^6Li in the 200 cm slab and at 0% in the 100 cm slab. This result offers some interesting possibilities. From Figs. 13 and 14 one can see that the optimum concentration of ^6Li for breeding purposes can be determined by adjusting the width of the slab. If this is true, it might be possible to design a breeding blanket with a proper width to give optimum breeding conditions for natural lithium. This would require no enrichment of ^7Li and could, of course, be a great economical asset to the fusion reactor. The results of Fig. 12, though, show that except for increasing the optimum concentration of the blanket very little increase in the total tritium breeding would occur by increasing the width of the slab past 100 cm. Thus, the ideal width will depend upon several factors. One would be the economics of an enrichment process for lithium. Another important consideration would be the physical problems associated with placing a blanket of lithium near the magnetic field lines which confine the plasma. Problems in this area could restrict the maximum blanket width which could be used. Therefore, an ideal

blanket width would have to take into account the effect of all these factors.

These results, regretfully, should be applied with reservations. The inadequacies of diffusion theory at high energies may have injected considerable errors into the calculations since the differential scattering cross section is highly anisotropic. Also, due to the way in which the groups were chosen, which resulted in 50% of the tritium being bred in group 2, even more accuracy is sacrificed. Upon further analysis of the data it was found that assuming N_7 to be constant was also a source of error. The correct treatment would be to use $N_t = 0.0378 \times 10^{24}$ atoms per cm^3 , where

$$N_t = N_6 + N_7 ,$$

and thus,

$$N_7 = \frac{N_t}{R + 1} . \quad (29)$$

This, of course, will affect all macroscopic cross sections and diffusion coefficients. The effect upon Figs. 13 and 14, due to the changes that this correction will make on the macroscopic cross sections, will only involve a scaling factor. The effect due to the errors in the diffusion coefficient, however, will not be scaled. A recalculation of D^1 using Eq. (29) for $R = 0.20$ resulted in $D^1 = 6.20$ cm. This is somewhat different than $D^1 = 5.15$ cm as shown in Fig. 10. Since the group diffusion coefficients are only used in leakage calculations, it is felt that the change in N_7 by using Eq. (29) will not affect the results appreciably. Also, since about 70% of the tritium is bred in groups 1 and 2, the errors in D^1 and D^2 will have the greatest

effect upon the total breeding rates. D^1 , however, was corrected in each case (see Fig. 10), and therefore, only the error in D^2 will affect the results. Figures 13 and 14 are the corrected results using Eq. (29).

It might be pointed out, however, that the way in which the cross sections were treated was shown to be adequate for this problem. Rather than using a flat probability distribution for the ${}^6\text{Li}(n, dn)$ and the ${}^7\text{Li}(n, tn)$ reactions, a bell-shaped distribution was tried. The resulting constants for the diffusion equation were calculated for a 100 cm slab with a concentration of 16.7% ${}^6\text{Li}$. A total breeding rate was calculated and found to be less than 2% off the total tritium breeding rate of the flat distribution.

To validate the assumption that all scattering was elastic, new cross sections were calculated ignoring the inelastic scattering. The total tritium breeding rate was calculated for a 100 cm slab with 16.7% ${}^6\text{Li}$ concentration and was found to be 22% off the total breeding rate found by treating the inelastic scattering as elastic. This, of course, would be the maximum possible error. The actual error would be considerably less.

Although some attempt was made to compensate for these errors, it is felt that a more accurate transport calculation should be made with a better choice of groups before any of these results can be applied. This study, however, could provide a good comparison for such a calculation.

VI. SUMMARY AND CONCLUSIONS

From the multi-group neutron diffusion code, FAIMOS, the fluxes for varying concentrations of ${}^6\text{Li}$ were calculated in two infinite slabs of lithium with widths of 100 cm and 200 cm. Using these fluxes, the total tritium breeding rates were calculated for each concentration and an optimum tritium breeding rate was found for each slab width.

In the 100 cm slab the optimum concentration of ${}^6\text{Li}$ was approximately 0%, or pure ${}^7\text{Li}$. When the slab width was increased, the optimum concentration rose to about 5% ${}^6\text{Li}$, which is almost natural lithium. This result suggests that it might be possible, by proper adjustment of the blanket width, to design a D-T fusion reactor blanket in which natural lithium would be the optimum condition for tritium breeding purposes. These results do not agree with El-Wakil [4] who suggested ${}^6\text{Li}$ enrichments in excess of 20%.

Although, from this study, the optimum tritium breeding rate occurred at about natural lithium concentration for the 200 cm slab, the author is hesitant to conclude this to be the ideal blanket width. From the flux calculations, it is evident that diffusion theory introduces errors, especially in the high energy ranges. Errors were also introduced from the way in which the groups were selected. As a result, it is hoped that the results of this study will be used in support of a more exact transport calculation, which in turn can lead to the design of a fusion blanket where the tritium breeding is utilized to its fullest extent.

VII. SUGGESTIONS FOR FURTHER STUDY

This study can be expanded and improved upon in several different ways. One of the first things that could be done would be to split the higher energy ranges into finer groups. This work only considered a slab width of 100 cm and 200 cm. Other widths could be tried. Other geometries, such as cylindrical or spherical, could also be used to study optimum concentrations. Rather than using diffusion theory, transport theory could be applied and then compared to the results of this study. The development of an enriching process for lithium and an economic analysis of such a process would also be a worthwhile and interesting extension of this work.

VIII. LITERATURE CITED

1. D. C. BALLER, "The FAIM Code, A Multigroup One-Dimensional Diffusion Equation Code," A.E.C. Report No. NAA-SR-7137 (1962).
2. GEORGE I. BELL, "Neutron Blanket Calculations for Thermonuclear Reactors," LA 3385, Contract W-7405-eng. 36, Los Alamos Scientific Laboratory, University of California, New Mexico (August 30, 1965).
3. ROBERT G. COCKRELL, "A Description of FAIMOS-A One-Dimensional Neutron Diffusion Equation Code," Boeing Huntsville Simulation Center, Boeing Company (1967).
4. M. M. EL-WAKIL, Nuclear Energy Conversion, International Textbook Co., Scranton, Pa. (1971).
5. SAMUEL GLASSTONE and ALEXANDER SESONSKE, Nuclear Reactor Engineering, Van Nostrand Reinhold Co., New York (1967).
6. DONALD J. HUGHES and JOHN A. HARVEY, Neutron Cross Sections, U.S. Government Printing Office, Washington, D.C. (1955).
7. HERBERT S. ISBIN, Nuclear Reactor Theory, Reinhold Publishing Co., New York (1963).
8. IRVING KAPLAN, Nuclear Physics, 2 ed., Addison-Wesley Publishing Co., Inc., Reading, Massachusetts (1962).
9. JOHN R. LAMARSH, Nuclear Reactor Theory, Addison-Wesley Publishing Co., Inc., Reading, Massachusetts (1966).
10. C. M. LEDERER, J. M. HOLLANDER, and J. PERLMAN, Tables of Isotopes, 6 ed., John Wiley and Sons, Inc., New York (March 1968).
11. W. B. MYERS, W. M. WELLS, and E. H. CANFIELD, "Tritium Regeneration in a D-T Thermonuclear Reactor Blanket," UCID-4480, Contract W-7405 eng.-48, 19p. UC-20-4, California University, Livermore, Lawrence Radiation Laboratory (May 22, 1962).
12. D. J. ROSE, "Feasibility of Power by Nuclear Fusion," ORNL-TM-2204, Contract W-7405 eng.-26, Oak Ridge National Laboratory, Tennessee (May 28, 1968).
13. JOHN R. STEHN, MURREY D. GOLDBERG, BENJAMIN A. MUGURNO, and RENATE WEINERCHASMAN, "Neutron Cross Sections," BNL 325, Vol. 1, Z=1 to 20, 2 ed., Supplement 2, U.S. Government Printing Office, Washington, D.C. (May 1964).

14. DON STEINER, "Neutronics Calculations and Cost Estimates for Fusion Reactor Blanket Assemblies," ORNL-TM-2360, 18p. 20-4 UNLTD Dist., Oak Ridge National Laboratory, Tennessee (November 22, 1968).

IX. ACKNOWLEDGMENTS

The author would like to express his sincere gratitude to Dr. Agust Valfells and Dr. Alfred F. Rohach of the Department of Nuclear Engineering for their guidance and helpful encouragement in the preparation of this work. I also gratefully acknowledge Argonne National Laboratory in supplying the computer code for use in this work.

I would also like to express my gratitude to my wife, Glynace, for her help in assembling the thesis.